Air Pollution from Forest and Vegetation Fires in Southeast Asia Disproportionately Impacts the Poor

Carly Lauren Serena Reddington[1], Luke Conibear[1], Suzanne Robinson[1], Christoph Knote[2], Steve Robert Arnold[3], and Dominick Vincent Spracklen[3]

[1]Institute for Climate and Atmospheric Science, School of Earth and Environment, University of Leeds
[2]Faculty of Medicine, University of Augsburg, Germany
[3]University of Leeds

November 23, 2022

Abstract

Forest and vegetation fires, used as tools for agriculture and deforestation, are a major source of air pollutants and can cause serious air quality issues in many parts of Asia. Actions to reduce fire may offer considerable, yet largely unrecognised, options for rapid improvements in air quality. In this study, we used a combination of regional and global air quality models and observations to examine the impact of forest and vegetation fires on air quality degradation and public health in Southeast Asia (including Mainland Southeast Asia and south-eastern China). We found that eliminating fire could substantially improve regional air quality across Southeast Asia by reducing the population exposure to fine particulate matter ($PM_{2.5}$) concentrations by 7% and surface ozone concentrations by 5%. These reductions in $PM_{2.5}$ exposures would yield a considerable public health benefit across the region; averting 59,000 (95% uncertainty interval (95UI): 55,200-62,900) premature deaths annually. Analysis of subnational infant mortality rate data and $PM_{2.5}$ exposure suggested that $PM_{2.5}$ from fires disproportionately impacts poorer populations across Southeast Asia. We identified two key regions in northern Laos and western Myanmar where particularly high levels of poverty coincide with exposure to relatively high levels of $PM_{2.5}$ from fires. Our results show that reducing forest and vegetation fires should be a public health priority for the Southeast Asia region.

Air Pollution from Forest and Vegetation Fires in Southeast Asia Disproportionately Impacts the Poor

Carly L. Reddington*[,1], Luke Conibear[1], Suzanne Robinson[1], Christoph Knote[2], Stephen R. Arnold[1], and Dominick V. Spracklen[1]

[1] Institute for Climate and Atmospheric Science, School of Earth and Environment, University of Leeds, Leeds, UK

[2] Model-Based Environmental Exposure Science, Faculty of Medicine, University of Augsburg, Germany

* Corresponding author: Carly Reddington (C.L.S.Reddington@leeds.ac.uk)

Key Points:

- Eliminating forest and vegetation fires could substantially improve regional air quality in Mainland Southeast Asia.
- Reducing exposure to particulate and ozone pollution from fires would yield a considerable public health benefit across Southeast Asia.
- Particulate air pollution from fires disproportionately impacts poorer populations across Southeast Asia.

Abstract

Forest and vegetation fires, used as tools for agriculture and deforestation, are a major source of air pollutants and can cause serious air quality issues in many parts of Asia. Actions to reduce fire may offer considerable, yet largely unrecognised, options for rapid improvements in air quality. In this study, we used a combination of regional and global air quality models and observations to examine the impact of forest and vegetation fires on air quality degradation and public health in Southeast Asia (including Mainland Southeast Asia and south-eastern China). We found that eliminating fire could substantially improve regional air quality across Southeast Asia by reducing the population exposure to fine particulate matter ($PM_{2.5}$) concentrations by 7% and surface ozone concentrations by 5%. These reductions in $PM_{2.5}$ exposures would yield a considerable public health benefit across the region; averting 59,000 (95% uncertainty interval (95UI): 55,200-62,900) premature deaths annually. Analysis of subnational infant mortality rate data and $PM_{2.5}$ exposure suggested that $PM_{2.5}$ from fires disproportionately impacts poorer populations across Southeast Asia. We identified two key regions in northern Laos and western Myanmar where particularly high levels of poverty coincide with exposure to relatively high levels of $PM_{2.5}$ from fires. Our results show that reducing forest and vegetation fires should be a public health priority for the Southeast Asia region.

1 Introduction

Forest and vegetation fires, also referred to as open biomass burning, are a major source of particulate matter (PM) (Chen et al., 2017), ozone (Jaffe and Wigder, 2012), and other air pollutants to the atmosphere and can cause serious air quality issues in many parts of East Asia (Marlier et al., 2012; Reddington et al., 2014; Koplitz et al., 2016; Crippa et al., 2016; Lee et al., 2018; Kiely et al., 2020; Bruni Zani et al., 2020). Observations show that emissions from these fires, which include agricultural residue burning and deforestation fires, influence pollutant concentrations in both rural and urban regions (Janjai et al., 2009; Pengchai et al., 2009; Tsai et al., 2013; Zhu et al., 2016; Lasko et al., 2018; Nguyen et al., 2019). Exposure to smoke from fires is associated with adverse health outcomes including morbidity and mortality (Jayachandran, 2009; Jacobson et al., 2014; Pongpiachan & Paowa, 2015; Reid et al., 2016; de Oliveira Alves et al., 2017; Pienkowski et al., 2017; Johnston et al., 2019; Vajanapoom et al., 2020). Most previous work has focussed on the air quality impacts of fires in Indonesia (Equatorial Asia) (Marlier et al., 2012; Reddington et al., 2014; Crippa et al., 2016; Koplitz et al., 2016; Kiely et al., 2020; Bruni Zani et al., 2020) and the Amazon (Reddington et al., 2015; Butt et al., 2020; Nawaz and Henze, 2020). In this study, we focus on the air quality impacts of fires in Mainland Southeast Asia (Myanmar, Thailand, Cambodia, Lao People's Democratic Republic (hereafter Laos), and Vietnam; also referred to as the Indochina Peninsula or Peninsula Southeast Asia) and south-eastern China, which have been much less studied.

In Southeast Asia, fires are used as a tool for agricultural management e.g., to remove agricultural residues (mainly from rice and sugarcane cultivation) and weeds, and for forest clearance for agricultural purposes (Biswas et al., 2015; Chen et al., 2017; Phairuang et al., 2017). Fires in Mainland Southeast Asia mainly occur during the pre-monsoon season (roughly February to April), due to widespread forest fires and crop residue burning in preparation for planting at the Asian summer monsoon onset (Huang et al., 2016; Phairuang et al., 2017). The increased fire activity coincides with a widespread stable temperature inversion layer over Thailand, Vietnam, Laos and Southern China (Nodzu et al., 2006) with hot, dry and stagnant air over northern Thailand (Kim Oanh & Leelasakultum, 2011) promoting haze conditions. During the burning season, long-range transport of smoke from fires in Mainland Southeast Asia has been observed in Southwest China (Zhu et al., 2016), south-eastern Tibetan Plateau (Sang et al., 2013), Southern China, Taiwan, and Hong Kong (Huang et al., 2013). Fires reduce substantially after the onset of the summer monsoon rainfall (in late April) and are minimal until around the start of the dry season (in November). Fires in this region display a degree of interannual variability linked to changes in atmospheric circulation features, such as the India-Burma Trough (Huang et al., 2016).

Several studies have used a mix of models and observations to explore the impacts of fire on atmospheric aerosol properties, visibility, and/or air quality in Mainland Southeast Asia (Lin et al., 2013; Huang et al., 2013; Duc et al., 2016; Lee et al., 2017; 2018; Li et al., 2017; Yin et al., 2019; Vongruang & Pimonsree, 2020). However, studies quantifying the contribution of fire to particulate air pollution, population exposure and public health are lacking in this region (Yadav et al., 2017; Johnston et al., 2019), compared in particular to the large number of studies focussed on Equatorial Asia (e.g., Marlier et al., 2012; Koplitz et al., 2016; Crippa et al., 2016; Kiely et al., 2020). Recent studies show that fire is the dominant cause of the variation of local ambient air quality in Mainland Southeast Asia (Yin et al., 2019); contributing 49% of ambient PM_{10} (particulate matter with aerodynamic diameter $\leq$ 10 μm) concentrations during peak open burning in March 2012 (Vongruang & Pimonsree, 2020) and 70%-80% to aerosol optical depth in source regions during March-April 2013 (Li et al., 2017). Preventing fire could yield substantial reductions in population-weighted $PM_{2.5}$ (particulate matter with aerodynamic diameter $\leq$ 2.5 μm) concentrations across Mainland Southeast Asia (Reddington et al., 2019a). There are large uncertainties associated with quantifying and simulating particulate emissions from fire in tropical regions (Reddington et al., 2016). In Mainland Southeast Asia, there is a large range in emissions estimates (Wiedinmyer et al., 2011; Kaiser et al., 2012; Shi & Yamaguchi, 2014; Sornpoon et al, 2014; Lasko et al., 2017; van der Werf et al., 2017; Phairuang et al., 2017) and varying performance when tested in models against observations (Fu et al., 2012; Reddington et al., 2014; 2016; Lee et al., 2017; Vongruang et al., 2017; Pimonsree et al., 2018; Takami et al., 2020). Emissions from the Fire Inventory from NCAR (FINN; Wiedinmyer et al., 2011) have been used widely in models over this region; with simulated PM concentrations showing good agreement against observations in some studies (Reddington et al., 2014; 2016; Takami et al., 2020), but overestimation by a factor of ~2 in others (Vongruang et al, 2017; Li et al., 2017; Pimonsree et al., 2018). Fires also impact ozone concentrations, being a source of ozone precursors and altering photochemistry, impacting ozone production (Jaffe and Wigder, 2012). The efficacy of photochemical ozone production in fire plumes is highly variable and uncertain, and is affected by non-linear ozone dependence on changes in precursor concentrations, and high particulate loadings, which affect photochemistry (Jaffe and Wigder, 2012). Fires have been shown to enhance regional ozone concentrations in Mainland Southeast Asia (Pochanart et al., 2001) and aloft over southern China (Chan et al., 2000; Chan et al., 2003; Kondo et al., 2004), although fires have also been implicated in suppressed ozone in some situations (Deng et al., 2008).

Links between socioeconomic factors, population exposure to ambient air pollution, and associated health effects have been well documented in parts of North America and Europe (e.g., Hajat et al., 2015; Fairburn et al., 2019). However, few studies have focussed on countries in Southeast Asia, with some demonstrating strong connections between ambient air pollution and poverty e.g., in urban areas of Laos (Dasgupta et al., 2005), rural areas of Vietnam (Narloch & Bangalore, 2018) and Ho Chi Minh City (Mehta et al., 2014); and others finding only weak connections e.g., in Cambodia and Vietnam (Dasgupta et al., 2005) or no connection e.g., in Laos (Pasanen et al., 2017). The majority of these studies explored links between poverty and multiple environmental risks, including ambient air pollution from all sources. To our knowledge, no previous studies have examined the poverty levels of populations exposed to air pollution from fires in this region.

In this work, we use a combination of satellite-derived datasets of fire emissions, models and observations to quantify the contribution of forest and vegetation fires to air quality degradation and disease burden in Mainland Southeast Asia and south-eastern China. We also examine the poverty levels of the Southeast Asian population exposed to $PM_{2.5}$ pollution derived specifically from fire emissions.

2 Materials and Methods

Model	GLOMAP (v7)	WRF-Chem (v3.7.1)
Domain	Global	Regional: East Asia
Horizontal resolution	2.8° x 2.8	30 km x 30 km (~0.3° x 0.3°)
Vertical levels	30 (up to 10 hPa)	33 (up to 10 hPa)
Anthropogenic emissions	MACCity (Granier et al., 2011) for 2003-2010	EDGAR-HTAP2 (Janssens-Maenhout et al., 2015) for 2010
Fire emissions	FINN1.5, GFAS1.2, GFED4	FINN1.5
Meteorology	Driven by ECMWF fields	Nudged to NCEP GFS fields (NCEP, 2000; 2007)

Aerosol size distribution	Modal scheme (7 log-normal modes)	Sectional scheme (MOSAIC 4-bin; Zaveri et al., 2008)
Gas-phase chemistry	TOMCAT (Chipperfield, 2006)	MOZART-4 (Emmons et al., 2010)
Simulation year(s)	2003 - 2015	2014
Simulations	1) GLOMAP_nofire: fire emissions excluded. 2) GLOMAP_FINN: with FINN fire emissions. 3) GLOMAP_GFAS: with GFAS fire emissions. 4) GLOMAP_GFED: with GFED fire emissions.	1) WRFChem_nofire: fire emissions excluded. 2) WRFChem_FINN: FINN fire emissions. 3) WRFChem_FINNx1.5: FINN fire emissions scaled upwards by a factor 1.5.

Table 1. Summary of the model setups for the GLOMAP global model and WRF-Chem regional model.

2.1 Description of the GLOMAP global aerosol model

We used the Global Model of Aerosol Processes (GLOMAP; Spracklen et al., 2005; Mann et al., 2010) to simulate multi-year (2003-2015) PM concentrations and evaluate the performance of three fire emissions datasets against observations. Table 1 summarises the model setup used for this study; see Sect. S1.1 and Reddington et al. (2016; 2019b) for further details.

2.1.1 Fire emissions in GLOMAP

Fire emissions of sulphur dioxide (SO_2), black carbon (BC) and organic carbon (OC) were specified using three different datasets: the National Centre for Atmospheric Research Fire Inventory version 1.5 (FINNv1.5) (Wiedinmyer et al., 2011), the Global Fire Emissions Dataset version 4.1 with small fires (GFED4s) (van der Werf et al., 2010; van der Werf et al., 2017) and the Global Fire Assimilation System versions 1.0 and 1.2 (GFASv1.0 and GFASv1.2) (Kaiser et al., 2012); hereafter referred to as FINN, GFED, and GFAS, respectively. The different fire emission estimation methodologies of these datasets are described in detail in their references given above and in our previous work (Reddington et al., 2016; 2019b). We use daily fire emissions from all three datasets (daily GFED emissions are available from 2003 onwards (Mu et al., 2011)). Fire emissions were distributed vertically over six ecosystem-dependent altitudes between the surface and 6 km according to Dentener et al. (2006). Over Mainland Southeast Asia, all emissions were injected below 3 km elevation, which is consistent with satellite observations of the vertical distribution of smoke in this region (Gautam et al., 2013).

2.1.2 GLOMAP model simulations

We performed four model simulations with GLOMAP: one simulation excluding fire emissions (“GLOMAP_nofire”); and three simulations each including a different fire emissions dataset (“GLOMAP_FINN”, “GLOMAP_GFED” and “GLOMAP_GFAS”). Simulations were run from 1st January 2003 to 31st December 2015 (after a 92-day spin-up), driven by ECMWF ERA-Interim global reanalyses (Dee et al., 2011) that correspond to the simulation date/time.

2.2 Description of the WRF-Chem regional model

We used the Weather Research and Forecasting model coupled with Chemistry (WRF-Chem; Grell et al., 2005) version 3.7.1, a high-resolution regional model, to simulate air pollutant concentrations for one year (2014) and quantify the public health impacts of long-term exposure to fire-derived $PM_{2.5}$ and ozone (O_3) concentrations. Table 1 summarises the model setup used for this study; see Sect. S1.2 for further details.

2.2.1 Fire emissions in WRF-Chem

Fire emissions were taken from FINN version 1.5 (Wiedinmyer et al., 2011), with a spatial resolution of 1 km x 1 km for the year 2014. Fire emissions were included for BC, OC, $PM_{2.5}$, PM_{10}, carbon monoxide, ammonia, nitrogen oxides, SO_2, and non-methane volatile organic compounds (speciated according to the Model for Ozone and Related Chemical Tracers (MOZART); Emmons et al., 2010). We applied a diurnal factor (Western Regional Air Partnership, 2005) to the daily emissions, which assumes greater emissions during the day (between 10:00 and 19:00 local time, peaking at 15:00-16:00 local time) and minimal emissions during the night. The injection heights of the fire emissions were calculated online in the model using the Freitas et al. (2007) plume-rise parameterisation. The plume-rise parameterisation applies a 1-D cloud-parcel model to each grid-column within the WRF-Chem model domain that contains a fire.

2.2.2 WRF-Chem model simulations

The model domain is located over East Asia, using a Lambert conformal conical projection with a horizontal resolution of 30 km x 30 km (covering a 130x124 grid) and 33 vertical levels up to a minimum pressure of 10 hPa. We re-gridded the model output, using linear interpolation, onto a regular latitude-longitude grid at 0.25° × 0.25° resolution. We performed three model simulations with WRF-Chem: one simulation excluding fire emissions ("WRChem_nofire"); one simulation including FINN fire emissions ("WRFChem_FINN"); and one simulation where FINN fire emissions of OC and BC were scaled upwards by a factor 1.5 ("WRFChem_FINNx1.5"). The simulation period was for one year from 9 January 2014 to 9 January 2015, with the first eight days of January 2014 run as spin-up. We selected 2014 for our simulation year since both PM and O_3 measurements are available for this year (Sect. 2.5).

2.3 Public health impact assessment

We estimated the disease burden attributable to ambient $PM_{2.5}$ exposure (simulated by WRF-Chem) using population attributable fractions of relative risk. The relative risk of disease at a specific ambient $PM_{2.5}$ exposure was estimated through the Global Exposure Mortality Model (GEMM) (Burnett et al., 2018). We calculated the disease burden due to long-term exposure to ambient O_3 (simulated by WRF-Chem) using the exposure-response function from Turner et al., (2016). Uncertainty intervals at the 95% confidence level (95UI) were estimated through using the derived uncertainty intervals from the exposure-outcome functions, baseline mortality and morbidity rates, and population age fractions. See Sect. S1.3 for further details.

The mortality due to fire emissions (M_{FIRE}) was calculated using the "subtraction" method (Conibear et al., 2018); calculating the difference between the premature mortality from all sources (M_{ALL}) and the premature mortality when fire emissions have been removed ($M_{\mathrm{FIRE\_OFF}}$) as in Eq. 1:

$$M_{\mathrm{FIRE}} = M_{\mathrm{ALL}} - M_{\mathrm{FIRE\_OFF}} \quad (1)$$

2.4 Poverty proxy data

As a proxy for population poverty levels, we used gridded subnational Infant Mortality Rate (IMR) estimates from NASA Socioeconomic Data and Applications Center for 2015 (Center for International Earth Science Information Network (CIESIN), 2018a). For further details see Sect. S1.5 and Fig. S8.

The IMR is defined as the number of children who die before their first birthday for every 1,000 live births in a given year. For context, previous studies have defined populations with IMR <15 to be not poor; 15 ≤ IMR < 32 to be moderately poor; 32 ≤ IMR < 65 to be poor; and 65 ≤ IMR < 100 to be very poor (De Sherbinin, 2008); and populations with a high IMR as having > 32 deaths per 1,000 live births (Barbier & Hochard, 2019).

Subnational IMR estimates have been used as a proxy for poverty indicators in a range of previous studies (De Sherbinin, 2008; Barlow et al., 2016; Barbier & Hochard, 2018; 2019; Hauenstein et al., 2019). A strong correlation between IMR and other poverty-related metrics, including population income, education and health (Reidpath & Allotey, 2003; De Sherbinin, 2008; O'Hare et al., 2013; Fritzell et al., 2015; Sartorius & Sartorius, 2014), justifies the use of IMR as a proxy for overall poverty levels. In addition, it is difficult to obtain alternative poverty measures at sub-national levels for mutilple countries (Dasgupta, 1993; CIESIN, 2018b). Other advantages of this dataset over alternative poverty measures include its highly standardised nature and availability for ≥90% of medium- and low-income country populations (Balk et al., 2006; CIESIN, 2018b).

2.5 Particulate matter and ozone measurements

We used 2003-2015 monthly mean PM_{10} concentrations measured at air quality monitoring stations located in fire-influenced regions of Thailand (Fig. S1a) from the Pollution Control Department (PCD) of the Thailand Government Ministry of Natural Resources and Environment. The fire-influenced stations were selected using GLOMAP or WRF-Chem model data where fire emissions contributed 20% or greater to the simulated annual mean PM_{10}. We used surface O_3 concentration measurements from air quality monitoring stations located in China and surrounding countries (Fig. S1b) from the Berkley Earth China Air Quality Data Set (Rohde & Muller, 2015). See Sect. S1.4 for further details on the measurements.

To evaluate model-simulated surface PM_{10} concentrations due only to the influence of fire, we calculated and compared simulated and measured fire-derived (smoke) PM_{10} concentrations. The simulated and measured fire-derived PM_{10} concentrations were estimated for each year separately, by subtracting the minimum monthly mean PM_{10} concentration from all monthly mean concentrations for that year. A similar approach has been used in previous modelling studies (e.g., Kiely et al., 2020) to isolate enhancements in surface PM concentrations due only to fires.

To quantify the agreement between model and observations, we used the Pearson correlation coefficient (r) and normalised mean bias factor (NMBF) as defined by Yu et al.

(2006). A positive NMBF indicates the model overestimates the observations by a factor of NMBF+1. A negative NMBF indicates the model underestimates the observations by a factor of 1–NMBF.

3 Results

3.1 Analysis of fire emissions over Southeast Asia

Figure 1 shows the 2003-2015 average spatial distribution of OC emissions from fire over Southeast Asia from GFAS, FINN and GFED. In all datasets greatest emissions occur in the northern regions of Laos, Cambodia, and Thailand, eastern and western Myanmar and southern Bangladesh, and lower emissions in central regions of Myanmar and Thailand, northern Vietnam and south-eastern China. The regions of greatest OC emissions are dominated by deforestation and degradation fires (as classified by GFED4; van der Werf et al., 2017; Fig. 1d). FINN generally estimates greatest OC emissions of the three emission datasets across the region, with lowest OC emissions estimated by GFED.

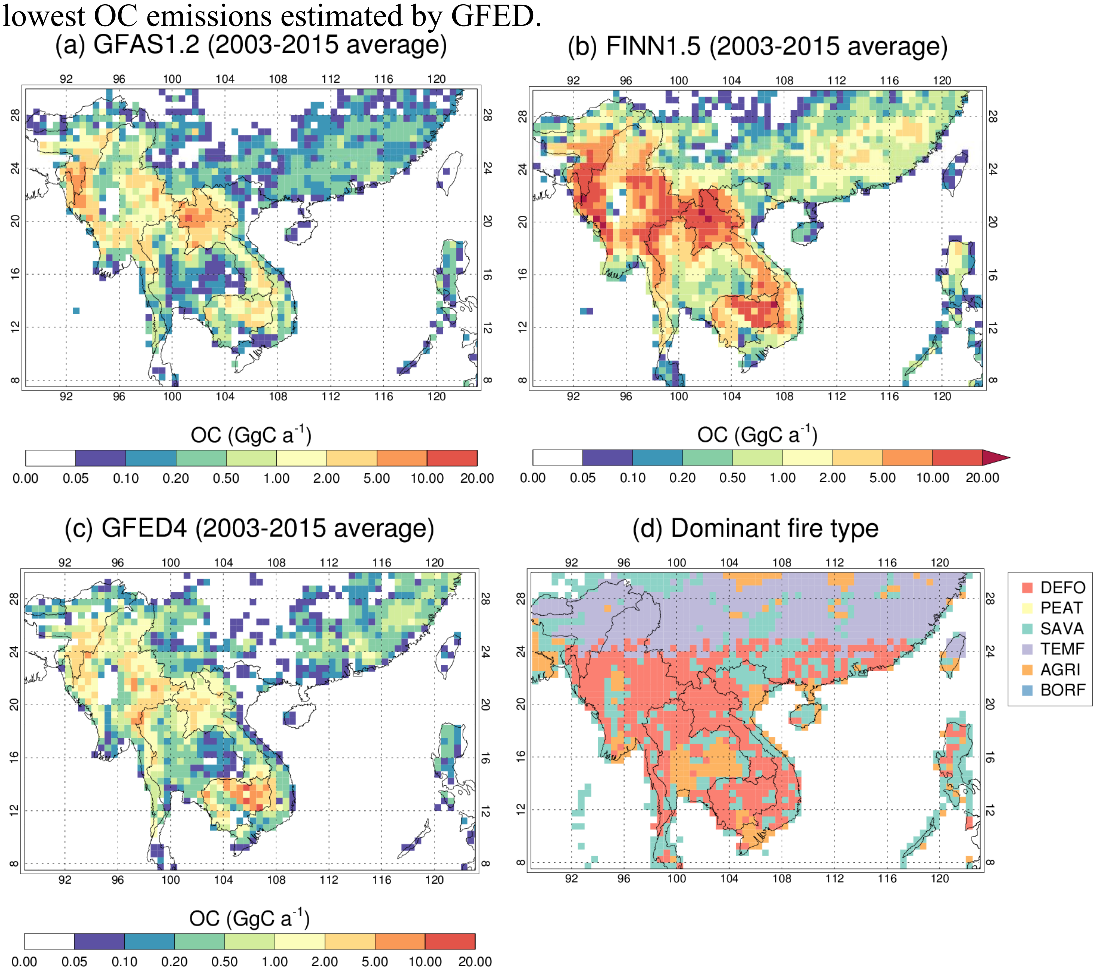

Figure 1. (a-c) Annual total organic carbon (OC) emissions from fire across Southeast Asia, averaged over the period (2003-2015) from three fire emission datasets: **(a)** GFAS version 1.0 (and version 1.2 from 2012 onwards), **(b)** FINN version 1.5 and **(c)** GFED version 4.1s (GFED4). Fire emissions are all re-gridded to 0.5° x 0.5° resolution for comparison. **(d)** Spatial distribution of the dominant fire types for fire emissions of OC for 2003-2015. Data is from GFED4 (van der Werf et al., 2010) re-gridded to 0.5° x 0.5° resolution. Fires are characterised into six types: Deforestation and degradation fires (DEFO); Peatland fires (PEAT); Savanna, grassland, and shrubland fires (SAVA); Temperate forest fires (TEMF); Agricultural waste burning (AGRI); and

Boreal forest fires (BORF). The dominant fire type was derived by calculating the maximum GFED4 OC emissions flux for each fire type in each 0.5°x0.5° grid cell over the period 2003-2015.

Figure 2 shows the 2003-2015 average annual OC emissions at the country scale with the greatest emissions from Myanmar and lowest from Vietnam. Countrywide FINN OC emissions are a factor 2-7 greater than GFED and a factor 3-5 greater than GFAS. Annual OC emissions summed across the region vary by a factor of 4 (GFAS: 0.90 Tg a^{-1}; FINN: 3.67 Tg a^{-1}; GFED: 0.87 Tg a^{-1}) and contribute between 5% (GFAS) and 18% (FINN) of 2003-2015 average global fire OC emissions. The importance of particulate fire emissions in this region depends on the fire emissions dataset used. In the FINN dataset, domain-wide fire OC emissions (3.7 Tg a^{-1}) are comparable to long-term average annual fire OC emissions in northern South America (3.1 Tg a^{-1}; Butt et al., 2020).

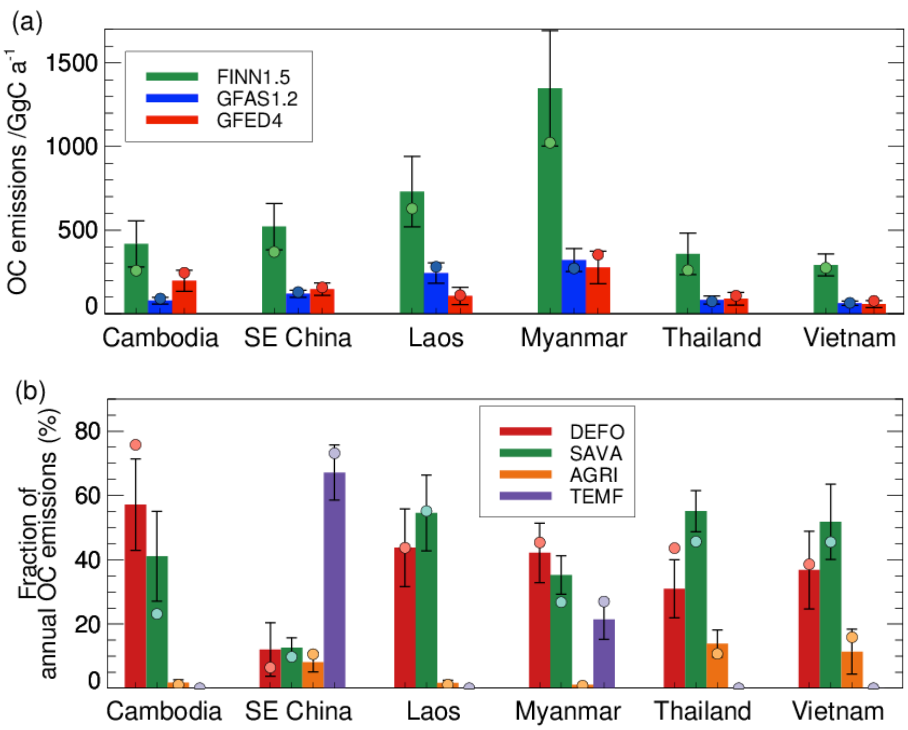

Figure 2. (a) Annual total organic carbon (OC) emissions from fire for countries/regions in Southeast Asia. Bars show annual total emissions averaged over the period (2003-2015) with error bars showing the standard deviation; circles show annual total emissions for 2014. OC emissions are shown from three fire emission datasets: GFAS version 1.0 (and version 1.2 from 2012 onwards), FINN version 1.5 and GFED version 4.1s (GFED4). "SE China" is defined as south of 30°N and east of 98°W. **(b)** Fire type fraction of GFED4 annual total OC emissions for four different fire types: Deforestation and degradation fires (DEFO); Savanna, grassland, and shrubland fires (SAVA); Agricultural waste burning (AGRI); and Temperate forest fires (TEMF) (van der Werf et al., 2010). Bars show fire type fractions averaged over the period (2003-2015) with error bars showing the standard deviation; circles show fire type fractions for 2014.

Differences in the magnitude of OC emissions estimated by the three datasets arise from multiple factors involved in the different fire detection and emission estimation methods used e.g., differences in the land use/land cover classifications used and the emissions factors assumed for various fire types and aerosol species (Liu et al., 2020); and possible biases in regions of agricultural residue burning and small savanna/grassland fires (Randerson et al., 2012; T. Zhang et al., 2018).

Across Mainland Southeast Asia, fire emissions are predominantly from deforestation/degradation fires (accounting for 31-57%) and savanna type fires (accounting for 35-55%) (Fig. 2b). A detailed analysis of forest fires in Myanmar confirms that most are of anthropogenic origin (Biswas et al., 2015). Vadrevu et al. (2019) found that most fires occurred in forests as opposed to cropland across much of Mainland Southeast Asia including Myanmar, Laos, Cambodia and Vietnam. In regions with both deforestation and savanna fires, deforestation fires emit a greater amount of particulate emissions, due to a combination of larger fuel loads/biomass consumption and emission factors, and thus tend to dominate emissions (Fig. 1d). However, savanna fires are more prevalent across the region and so the accumulated emissions from this fire type per country are generally comparable to or greater than deforestation fires. In south-eastern China, OC emissions arise predominantly from fires classified as temperate forest fires (67%). Agricultural fires make up a relatively small fraction of fire OC emissions across the region (1-14%), but the occurrence of these fires may be underestimated or misrepresented both in GFED (Reddington et al., 2016; T. Zhang et al., 2018), and more widely by satellite-based estimates (Zhang et al., 2016; Stavrakou et al., 2016; Lasko et al., 2017; Shen et al., 2019; Zhang et al., 2020).

3.2 Model evaluation

3.2.1 Evaluation of fire emissions datasets

Figure 3 compares three fire emissions datasets in GLOMAP against long-term surface measurements of PM_{10} from 12 fire-influenced stations in Thailand. The measurements show a consistent peak in monthly mean fire-derived PM_{10} concentrations of ~60-130 mg m^{-3} during the pre-monsoon season (roughly between January and May) across all years. Annual peak concentrations show a moderate degree of interannual variability, with relatively low peaks measured during 2003, 2008 and 2011 (and relatively high in 2004, 2007 and 2012). The multi-year GLOMAP simulations demonstrate that fires consistently make a substantial contribution to surface PM_{10} concentrations in northern Thailand over a 13-year period.

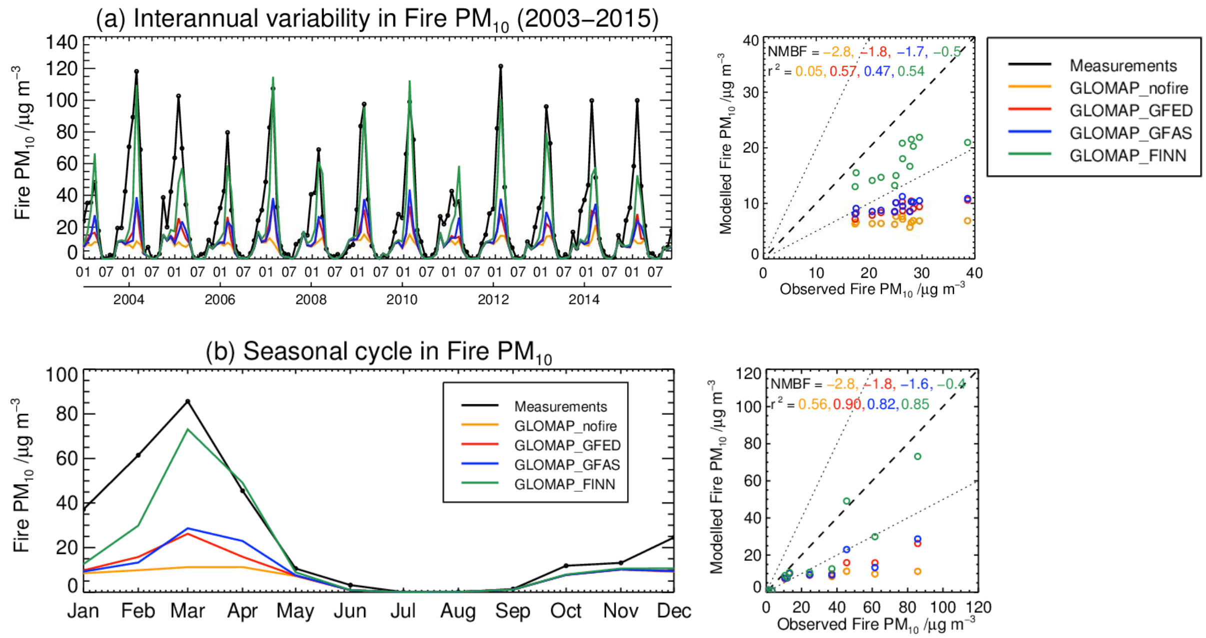

Figure 3. Evaluation of GLOMAP-simulated PM_{10} over Thailand. **(a)** Left: time-series of simulated and measured monthly mean fire-derived PM_{10} concentrations between 2003 and 2015, averaged over 12 fire-influenced stations (shown in Fig. S1a); Right: simulated versus measured annual mean fire-derived PM_{10}. **(b)** Left: time-series of simulated and measured multi-annual average seasonal cycle of fire-derived PM_{10} concentrations, averaged over the same stations as the upper panel; Right: simulated versus measured multi-annual monthly mean fire-derived PM_{10}. The model bias (NMBF) and correlation (r^2) between modelled and measured values are given at the top of the righthand figures. Simulated concentrations are shown for the model with FINN1.5 (GLOMAP_FINN), GFAS1.2 (GLOMAP_GFAS), GFED4 (GLOMAP_GFED) emissions, and without fire emissions (GLOMAP_nofire).

Figure 3a shows GLOMAP generally captures the measured interannual variability in fire-derived PM_{10} when fire emissions are included in the model (r^2=0.47-0.57, depending on the emission dataset) but underestimates the magnitude of the measurements in all simulations (NMBF=-1.8 to -0.5), particularly in 2005, 2014 and 2015. The smallest model bias in annual mean fire-derived PM_{10} across all years (NMBF=-0.5) is achieved with FINN emissions.

Figure 3b shows the strong seasonal variability in measured fire-derived PM_{10} concentrations, with average concentrations peaking in March and then decreasing to very low values between May and September. The measured seasonal variation is captured well in the simulations with fire emissions (r^2=0.82-0.90, depending on the emission dataset). However, the magnitude of fire-derived PM_{10} concentrations is best captured by the model with FINN emissions (Fig. 3b; NMBF=-0.4; see further analysis in Sect. S2.1 and Fig. S2). This result is consistent with our previous work (Reddington et al., 2016) that used AERONET aerosol optical depth to evaluate the GLOMAP model over Southeast Asia. Therefore, we use the FINN emissions in our high-resolution regional model simulations in the following sections.

3.2.2 Evaluation of WRF-Chem particulate matter concentrations

Figure 4 compares WRF-Chem simulated and measured regional-average seasonal cycles in fire-derived PM_{10} for 12 fire-influenced stations in Thailand during 2014. We note that annual fire emissions in FINN for 2014 are comparable to or lower than the 2003-2015 average (Fig. 2a). The model with FINN emissions well simulates the monthly mean variation in measured fire-derived PM_{10} concentrations (r^2=0.89) but underestimates the magnitude of the observations (NMBF=-0.28) predominantly during January to July. This is consistent with *total* PM_{10} concentrations (Fig. S3).

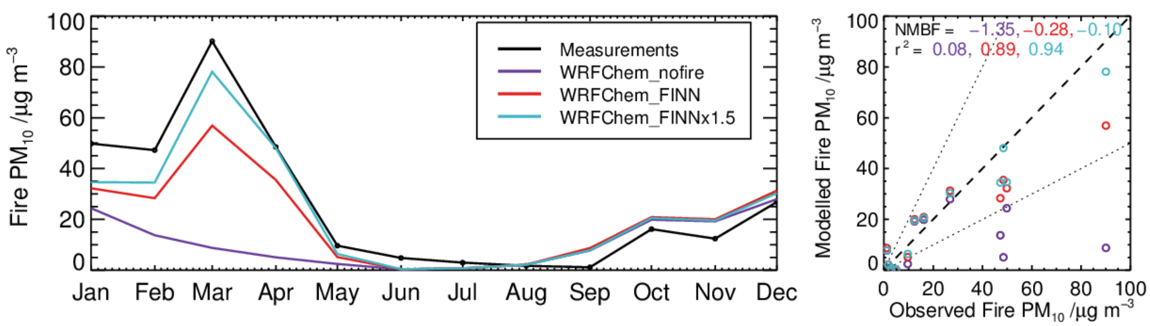

Figure 4. Evaluation of WRF-Chem-simulated PM_{10} over Thailand. Left: Time-series of simulated and measured monthly mean fire-derived PM_{10} concentrations during 2014 averaged over 12 fire-influencd stations (shown in Fig. S1a). Right: simulated versus measured annual mean fire-derived PM_{10}. The model bias (NMBF) and correlation (r^2) between modelled and measured values are given at the top of the righthand figure. Simulated concentrations are shown for the model without fire emissions (WRFChem_nofire), and for the model with FINN emissions (WRFChem_FINN) and with FINN emissions scaled upwards by a factor 1.5 (WRFChem_FINNx1.5).

Increasing the particulate fire emissions by a factor 1.5 improves the overall agreement with measured fire-derived PM_{10} (Fig. 4; r^2=0.94, NMBF=-0.10). Specifically, the FINNx1.5 simulation better captures the measured seasonal variation and magnitude of fire-derived PM_{10} at 11 out of 12 stations (Fig. S4; FINN: normalised standard deviation (NSD)=0.55-1.21; FINNx1.5: NSD=0.64-1.74), with little change in the strong temporal correlation (FINN: r=0.83-0.97; FINNx1.5: r=0.87-0.98). The FINNx1.5 simulation also agrees well with $PM_{2.5}$ measurements (see Sect. S2.2 and Fig. S5). Previous studies have used similar or larger scaling factors to increase fire emissions in models to better match observations (see Reddington et al. (2016) and references therein). In the following sections, we show results from the FINNx1.5 simulation as it gives the best match to PM observations.

3.2.3 Evaluation of WRF-Chem surface ozone concentrations

Figure 5 compares simulated and measured daily mean surface O_3 mixing ratios averaged over two regions in Southeast Asia during April to July 2014. Regional-average measured O_3 mixing ratios range from ~10 to ~60 ppbv. Variability in surface O_3 concentrations over Southeast Asia is driven by a complex mix of factors, including varying precursor gas emissions and concentrations, photochemical production, and meteorological effects (causing accumulation, transport and removal). We evaluate the model against total O_3 rather than fire-derived O_3, as for total $PM_{2.5}$ in Sect. S2.2, because these quantities are used for the health impact assessment in Sect. 3.4.

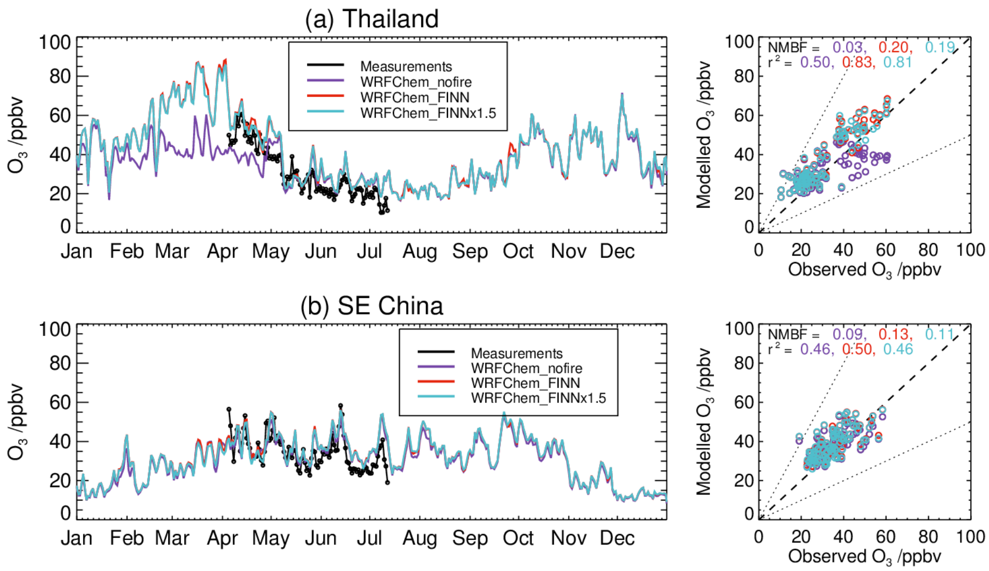

Figure 5. Evaluation of WRF-Chem-simulated ozone (O_3) over Thailand and South-eastern (SE) China. Left: Time-series of simulated and measured daily mean surface O_3 mixing ratios during 2014; Right: simulated versus measured daily mean O_3. Regional averages are shown for: **(a)** Thailand (9 air quality monitoring stations); and **(b)** SE China (368 stations in south-eastern Mainland China, 72 stations in Taiwan/Republic of China, and 12 stations in Hong Kong Special Administrative Region). O_3 measurements are available from April to July 2014. The model bias (NMBF) and correlation (r^2) between modelled and measured values are given at the top of the righthand figures. Simulated values are shown for three model simulations: without fire emissions (WRFChem_nofire); with FINN fire emissions (WRFChem_FINN); and with FINN emissions scaled upwards by a factor 1.5 (WRFChem_FINNx1.5).

Measured surface O_3 mixing ratios in Thailand show a peak during April (Fig. 5a), which has been reported to be due to regional scale O_3 production triggered by fires (Pochanart et al., 2001, Chen et al., 2017). The FINNx1.5 simulation captures this peak and reproduces the general daily variability in measured O_3 concentrations (r^2=0.81), while slightly overestimating the magnitude of the measurements (NMBF=0.19). In south-eastern China (Fig. 5b), the model simulates the magnitude and temporal variability of the measured O_3 mixing ratios reasonably well (r^2=0.46, NMBF=0.11). Model-measurement comparisons are shown for separate provinces/regions in south-eastern China in Fig. S6. Previous studies have reported increased ozone concentrations aloft (~2-6 km altitude) over southern China due to fires in Mainland Southeast Asia but show little enhancement at the surface (Chan et al., 2000; Chan et al., 2003; Kondo et al., 2004), consistent with the model results. Reductions in photochemical ozone production as a result of PM from fires can also act to reduce ozone concentrations (Deng et al., 2008).

3.3 Impacts of forest and vegetation fires on air quality

Figure 6a shows the relative change in simulated surface annual (2014) mean $PM_{2.5}$ concentration when fire emissions are excluded in WRF-Chem (see Fig. S7 for simulated annual mean surface concentrations). Eliminating fire emissions reduces simulated annual mean surface $PM_{2.5}$ concentrations by ~40-70% in northern Thailand, Myanmar, Cambodia and Laos, with reductions in south-eastern China ranging from ~10-40% in the region of Mainland Southeast Asia and in Taiwan, to ≤10% in the provinces further east. Population-weighted annual mean $PM_{2.5}$ concentrations across Southeast Asia are reduced by 7%, with reductions of 20% in Cambodia, 41% in Laos, 31% in Myanmar, 23% in Thailand, and 7% in Vietnam.

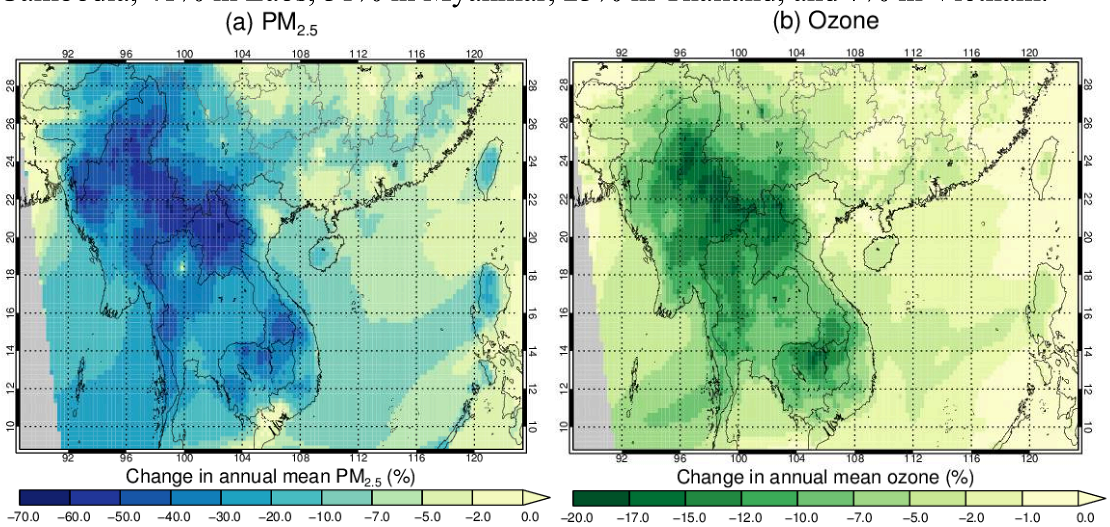

Figure 6. The air quality effects of eliminating fire across Southeast Asia. Shown are the percentage changes in WRF-Chem-simulated annual (2014) mean **(a)** $PM_{2.5}$ and **(b)** ozone concentrations at ground level when fire emissions are excluded in the model. Results are shown for the high fire emissions scenario (WRFChem_FINNx1.5). Regions in grey are outside the model domain.

Simulated $PM_{2.5}$ concentrations suggest that for 2014, the World Health Organization (WHO) Air Quality Guideline for $PM_{2.5}$ (an annual mean of 10 μg m^{-3}; WHO (2006)) is exceeded in almost every location in Southeast Asia even when fires are excluded (see Fig. S7a and S7b). However, excluding fires substantially reduces the population exposed to levels of $PM_{2.5}$ above the WHO Air Quality Interim Target 2 (annual mean of 25 μg m^{-3}) in Thailand (by 64%), Myanmar (by 100%), Laos (by 92%) and Cambodia (by 44%), with smaller reductions in Vietnam (by 9%) and south-eastern China (by 3%).

Figures 6b shows the relative change in simulated surface annual mean O_3 concentration when fire emissions are excluded from the model (see Fig. S7c and S7d for absolute concentrations). The spatial pattern of relative changes in surface O_3 is fairly consistent with the peak and minimum relative changes in surface $PM_{2.5}$ concentrations, with largest reductions over northern Thailand, Myanmar, Cambodia and Laos (up to 20%) and smaller reductions over most of south-eastern China (<15%). When fires are excluded from the model, the annual average daily maximum 8-hour (ADM8h) O_3 concentration is reduced by 5% across Southeast Asia, with reductions of 10% in Cambodia, 12% in Myanmar and Laos, 8% in Thailand, 5% in Vietnam, and 2% in south-eastern China.

3.4 Impacts of forest and vegetation fires on public health

Table 2 shows the averted disease burden due to changes in long-term exposure to ambient $PM_{2.5}$ and O_3 from eliminating fire emissions. Eliminating fire emissions reduces the annual disease burden from ambient $PM_{2.5}$ exposure by 12% in Mainland Southeast Asia (ranging from 5% in Vietnam to 28% in Laos), averting a total of 27,500 (95UI: 24,700-30,400) premature deaths. In south-eastern China, the disease burden is reduced by 3%, averting 31,400

(95UI: 30,500-32,400) premature deaths. Assuming a low fire scenario (FINN) decreases the averted annual $PM_{2.5}$ disease burden from eliminating fire emissions by a factor of 1.3 (Table S2).

Country/ region	Reduction in $PM_{2.5}$ exposure	Reduction in $PM_{2.5}$ MORT	$PM_{2.5}$ MORT (yr^{-1})	$PM_{2.5}$ DALYs (yr^{-1})	Reduction in O_3 exposure	Reduction in O_3 MORT	O_3 MORT (yr^{-1})
Cambodia	20%	13%	1,500 (1,300-1,700)	59,500 (49,100-71,700)	10%	15%	140 (130-160)
Laos	41%	28%	1,600 (1,300-1,800)	63,600 (49,400-77,400)	12%	16%	80 (70-80)
Myanmar	31%	21%	10,800 (9,500-12,000)	393,100 (326,200-467,300)	12%	20%	1,070 (940-1,190)
Thailand	23%	15%	8,500 (7,900-9,100)	344,500 (288,600-405,700)	8%	7%	600 (550-650)
Vietnam	7%	5%	5,100 (4,600-5,700)	186,800 (145,100-225,400)	5%	4%	360 (310-390)
SE China	5%	3%	31,400 (30,500-32,400)	1,042,900 (919,200-1,184,800)	2%	1%	1,530 (1,380-1,660)
Total Mainland SE Asia	16%	12%	27,500 (24,700-30,400)	1,047,500 (867,500-1,247,300)	9%	10%	2,250 (2,000-2,470)
Total SE Asia domain	7%	5%	59,000 (55,200-62,900	2,090,300 (1,786,700-2,432,200)	5%	3%	3,790 (3,380-4,130)

Table 2. Averted public health effects due to changes in long-term exposure to ambient $PM_{2.5}$ and ozone (O_3) from eliminating fire emissions. Shown are the percentage reductions in population weighted annual mean $PM_{2.5}$ concentration ($PM_{2.5}$ exposure), annual mean daily maximum 8-hour (ADM8h) O_3 concentration (O_3 exposure), and annual disease burden; and the numbers of averted annual premature mortalities (MORT) and disability-adjusted life years (DALYs) per country for the higher fire emissions scenario (FINNx1.5). Values in parentheses represent the 95% uncertainty intervals (95UI). $PM_{2.5}$ mortality values are rounded to the nearest 100 and O_3 mortality values are rounded to the nearest 10. “SE China” is defined as south of 30°N and east of 98°W, and includes Hong Kong SAR, Macau SAR and Taiwan. “Mainland SE Asia” includes Cambodia, Laos, Myanmar, Thailand, and Vietnam.

Figure 7 shows the averted annual premature mortalities and mortality rate by country from eliminating fire emissions. Whilst the number of avoided total premature mortalities is much higher in south-eastern China, due to the high population, the averted mortality rate in this region is smaller than the other countries, due to the more moderate impact of fire on air quality (Sect. 3.3). The greatest impact per capita is in Laos and Myanmar where 25 (95UI: 21-29) and 26 (95UI: 23-29) premature deaths per 100,000 head of population are averted per year, respectively. In Cambodia, Thailand, Vietnam and south-eastern China, the averted mortality rate ranges from 10 to 17 (95UI: 9-18) premature deaths per 100,000 people per year.

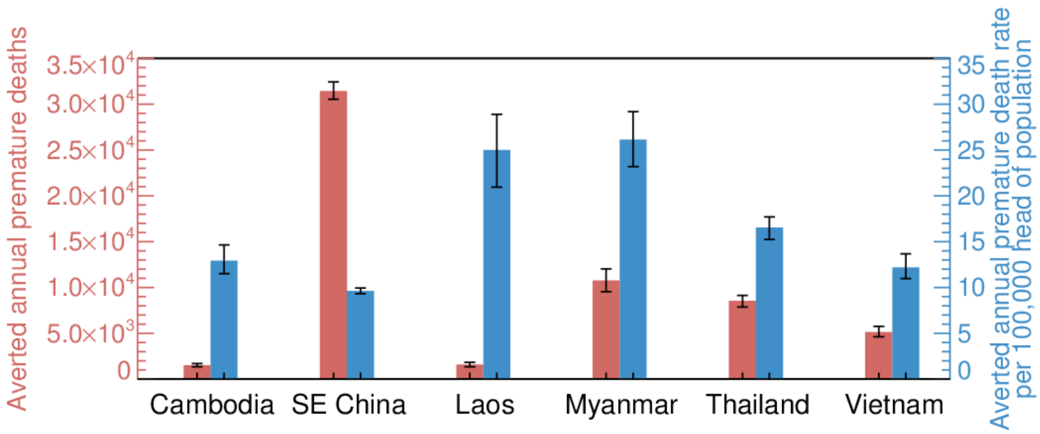

Figure 7. The number of averted annual premature mortalities across Southeast Asia due to changes in long-term exposure to ambient $PM_{2.5}$ from eliminating fire emissions. The total annual premature mortality estimates are shown for each country by the red bars; the annual premature mortality rate estimates (mortalities per 100,000 head of population) are shown for each country by the blue bars. Error bars represent the 95% uncertainty intervals.

Eliminating fire emissions reduces the annual disease burden due to long-term exposure to ambient O_3 by 10% in Mainland Southeast Asia (ranging from 4% in Vietnam to 20% in Myanmar), averting a total of 2,250 (95UI: 2,000-2,470) premature deaths (Table 2). In south-eastern China, the annual disease burden is reduced by 1%, averting 1,530 (95UI: 1,380-1,660) premature deaths. In the FINNx1.5 scenario, the reduction in surface O_3 by country is slightly smaller than for the FINN scenario due to non-linear effects driving O_3 concentrations, resulting in smaller averted disease burdens (Table S2).

3.5 Poverty and smoke exposure

In this section, we examine the poverty levels of the Southeast Asian population exposed to fire-derived $PM_{2.5}$ pollution. Figure 8 shows WRF-Chem simulated annual mean fire-derived (smoke) $PM_{2.5}$ and non-fire $PM_{2.5}$ concentrations plotted against gridded poverty proxy (IMR) data for the Southeast Asian domain. Populations in regions with relatively high IMRs (>60 deaths per 1,000 births) are generally exposed to higher annual mean $PM_{2.5}$ concentrations from fire than populations with relatively low IMRs (<40 deaths per 1,000 births). In areas with IMR $\geq$ 60, the mean fire-derived $PM_{2.5}$ exposure (10.6 $\mu g\ m^{-3}$) is significantly greater (at the 99% confidence level) than the mean fire-derived $PM_{2.5}$ exposure in areas with IMR $\leq$ 20 (3.5 $\mu g\ m^{-3}$). At the national scale, countries with higher IMRs (Laos, Cambodia, and Myanmar; Fig. S8) also experience greater particulate emissions from fires (Fig. 1b) and greater exposure to fire-derived $PM_{2.5}$ (Fig. 6a) than other countries in Southeast Asia. Also, this result may reflect that rural populations in Southeast Asia, which are generally located closer to forest and vegetation fires, often experience greater IMRs (e.g., Myanmar Ministry of Health, 2003).

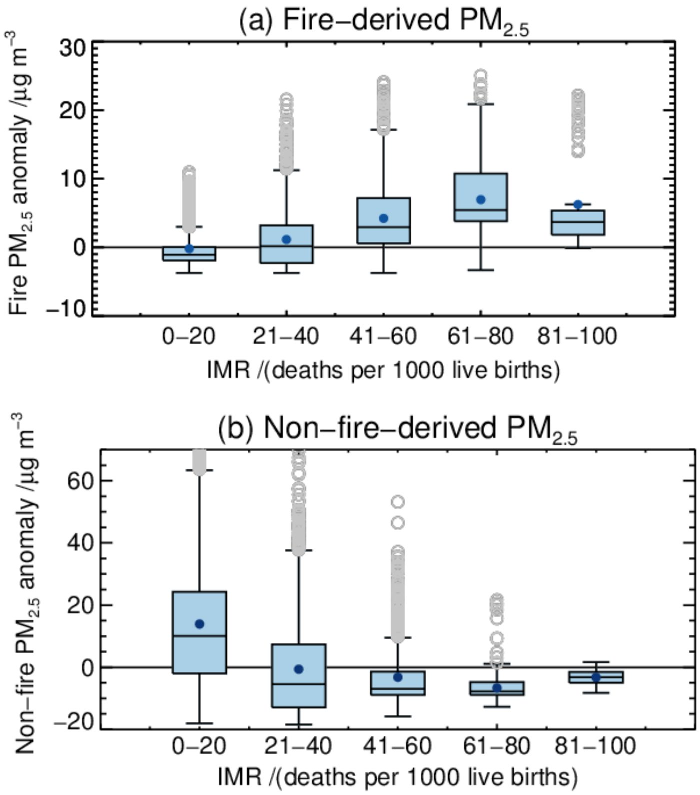

Figure 8. WRF-Chem simulated annual mean **(a)** fire-derived $PM_{2.5}$ and **(b)** non-fire-derived $PM_{2.5}$ concentrations versus binned subnational Infant Mortality Rate (IMR) values across the Southeast Asian domain. Shown are the simulated $PM_{2.5}$ anomalies i.e., the difference of the $PM_{2.5}$ concentration in each IMR bin from the mean $PM_{2.5}$ concentration across all IMR bins. Boxes enclose the interquartile range; filled circles show the mean; error bars extend to 1.5 times the 25^{th} and 75^{th} percentiles; grey open circles show outliers. Prior to analysis IMR values were regridded to the WRF-Chem grid by taking the mean gridded IMR value per 0.25°x0.25° grid cell.

When we consider $PM_{2.5}$ from all sources other than fires (Fig. 8b), we obtain the opposite result, where populations in regions with relatively high IMRs (>60 deaths per 1,000 births) are generally exposed to lower annual mean non-fire $PM_{2.5}$ concentrations than populations with relatively low IMRs (<40 deaths per 1000 births). In areas with IMR $\geq$ 60, the mean non-fire $PM_{2.5}$ exposure (15.1 μg m^{-3}) is significantly lower (at the 99% confidence level) than the mean non-fire $PM_{2.5}$ exposure in areas with IMR $\leq$ 20 (35.3 μg m^{-3}).

Considering $PM_{2.5}$ from all sources (Fig. S9), we find that on average, ‘not poor’ and ‘moderately poor’ populations (with IMR < 32) are exposed to annual mean $PM_{2.5}$ concentrations derived predominantly (88%) from non-fire sources. However, for ‘very poor’ populations (with 65 ≤ IMR < 100), fire-derived $PM_{2.5}$ makes up a more substantial fraction (41%) of the total $PM_{2.5}$ exposure, with 59% from non-fire sources.

Figure 9 shows the spatial distribution of relative poverty levels (IMR) and fire-derived $PM_{2.5}$ exposure (WRF-Chem-simulated annual mean fire-derived $PM_{2.5}$ concentrations) across Southeast Asia. This figure indicates a large region in Southeast Asia (including northern Laos, north-west Vietnam, northern Cambodia, northern and eastern Myanmar, and Yunnan province in China) where populations with medium or high levels of poverty are exposed to medium or high levels of $PM_{2.5}$ pollution from fires. In particular, two areas in northern Laos and western Myanmar show relatively high levels of both poverty and $PM_{2.5}$ exposure, suggesting populations in these regions may be particularly at risk to health impacts from fires.

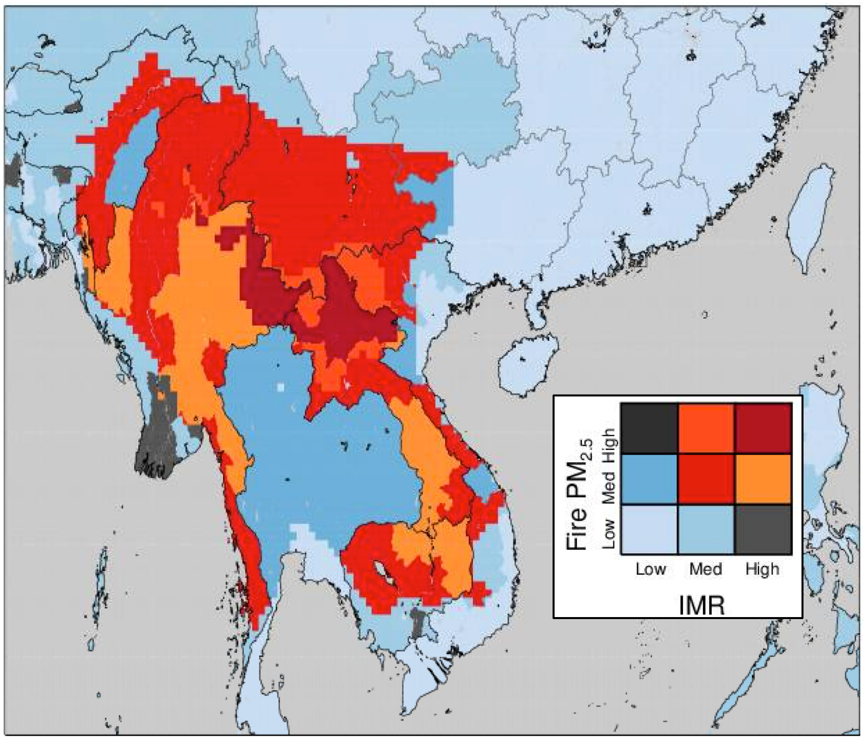

Figure 9. Spatial distribution of poverty proxy data (infant mortality rate (IMR) estimates) and WRF-Chem-simulated annual mean fire-derived $PM_{2.5}$ concentrations across Southeast Asia. Poverty proxy (IMR) ranges are: Low: 0-20; Med=20-60; High=60-100 deaths per 1,000 live births. $PM_{2.5}$ concentration ranges are: Low=0-5 $\mu g\ m^{-3}$; Med=5-15 $\mu g\ m^{-3}$; High=15-30 $\mu g\ m^{-3}$.

Overall, these results suggest that populations with greater levels of poverty are disproportionally exposed to $PM_{2.5}$ from vegetation and forest fires in Southeast Asia. For very poor populations, fire-derived $PM_{2.5}$ concentrations contribute over a third to the total $PM_{2.5}$ exposure.

4 Discussion of public health impacts and policy

To put our estimated public health impacts into context, we compare disease burdens due to fire-derived $PM_{2.5}$ exposure calculated for other fire-intensive regions. Previous studies have estimated that preventing forest and vegetation fires would avert ~5,000-16,800 annual premature deaths across South America (Johnston et al., 2012; Reddington et al., 2015; Butt et al., 2020; Nawaz & Henze, 2020) and ~6,000-100,300 annual premature deaths across Equatorial Asia (Marlier et al., 2012; Crippa et al., 2016; Koplitz et al., 2016; Kiely et al., 2020). The wide range in estimates reflects differences in the experimental design/methods e.g., time periods (with strong interannual variability in fire emissions in these regions), atmospheric models, and, in particular, exposure-outcome associations (as discussed by Conibear et al., 2018; Reddington et al., 2019a; Butt et al., 2020; Kiely et al., 2020; Giani et al., 2020).

Using similar WRF-Chem setups and exposure-outcome association (the GEMM) as used in this study, previous studies found that eliminating fire would avert 16,800 (95UI: 16,300-17,400) premature deaths across South America in 2012 (Butt et al., 2020) and 44,000 (34,700-53,900) premature deaths across Equatorial Asia in 2015 (Kiely et al., 2020). The total averted disease burden for our Southeast Asian domain, 59,000 (95UI: 55,200-62,900) premature deaths, is greater than estimated for the other two fire-influenced regions, despite there being a major drought-induced haze event across Equatorial Asia in 2015. Removing the population size dependence, the per capita averted disease burden estimates for countries in Southeast Asia (10-26 (95UI: 9-29) deaths per 100,000 people) are comparable to those estimated for Bolivia, Brazil and Peru (11-22 (95UI: 10-26) deaths per 100,000 people) in 2012 (Butt et al., 2020) and for Singapore, Brunei and Malaysia (20-33 (95UI: 16-41) deaths per 100,000 people) in 2015 (Kiely et al., 2020). These comparisons indicate that populations in Mainland Southeast Asia, suffer from substantial exposure to smoke from fires with adverse impacts on public health that are comparable to other major fire regions in the tropics.

There is considerable uncertainty associated with deriving fire emissions from satellite retrievals (e.g., Reddington et al., 2016; Pan et al., 2020), and previous studies have reported that these emissions, particularly from agricultural fires, may be underestimated in Mainland Southeast Asia (Sornpoon et al., 2014; Reddington et al., 2016; Lasko et al., 2017) and China (Zhang et al., 2016; Stavrakou et al., 2016; Shen et al., 2019; Zhang et al., 2020). The underestimation of emissions from these fires is likely due to multiple factors, but particularly their small size (difficult for burned area products to detect) and short duration of active burning (a high potential to be missed by polar-orbiting satellites with detection frequencies of only a few times per day) (e.g., T. Zhang et al., 2018). Applying a simple scaling factor to the fire emissions will partly compensate for emissions underestimation, but emissions estimates are still likely to be conservative in regions with a high number of missed detections.

We compared the averted disease burden from eliminating fire to those that would be achieved by eliminating other emissions sectors, estimated in Reddington et al. (2019a). Using the same health impact calculation method as Reddington et al. (2019a) (the Integrated Exposure-Response function (GBD 2015 Risk Factors Collaborators, 2016)), the avoided $PM_{2.5}$ disease burdens in Mainland Southeast Asia due to eliminating fire emissions (12,200 (95UI: 6,500-19,000) premature deaths) are lower than calculated with the GEMM (Table 2). These values are comparable to eliminating all industrial emissions; a factor 6 greater than eliminating electricity generation emissions; and a factor 10 greater than eliminating land transport across Mainland Southeast Asia. We note that we do not account for toxicity variation within $PM_{2.5}$ exposure as it is currently unknown; with disagreement in the literature regarding the toxicity of fire-derived PM relative to ambient PM (Wegesser et al., 2009; Pongpiachan, 2016; Johnston et al., 2019; Aguilera et al., 2021). The health effects of different sources and components of PM exposure is an ongoing area of research (Naeher et al., 2007; Adetona et al., 2016; Liu et al., 2015; Reid et al., 2016).

Our analysis shows that a reduction of fire across southeast Asia would have substantial health benefits. Successful fire management requires information about the main types and causes of fire. Across Mainland Southeast Asia, emissions are dominated by forest fires (deforestation, savanna, and temperate forest classes in GFED) which account for 96% of particulate emissions across our domain, with greater contributions in Cambodia, Laos and Myanmar. A detailed analysis of fires confirms that most fires in the region occur in forest land covers (Vadrevu et al, 2019). A close association between fire and deforestation has also been shown in other tropical regions including the Brazilian Amazon (Reddington et al., 2015) and Indonesia (Adrianto et al., 2019; 2020). In Southeast Asia, fires are lit in forests to clear the land for agriculture (slash and burn, deforestation fires), to induce growth of grass for grazing, and for collection of forest products (Vadrevu et al., 2019). The large contribution of forest fires to particulate emissions suggests that reducing deforestation and associated fires should be a public health priority for the region. In Cambodia, deforestation has been linked to increased incidence of acute respiratory infection in children, likely due to increased exposure to smoke from deforestation fires (Pienkowski et al. 2017). Future work exploring the relative contributions of different fire types to air pollution in Mainland Southeast Asia would be useful to inform policy options to improve air quality.

Several policies have already been implemented to reduce agricultural fires in Southeast Asia e.g., an Alternative Energy Development Plan and a zero-burning policy for sugarcane in Thailand (Kumar et al., 2020). However, challenges remain with regards to the enforcement of these policies and their practicality, particularly for farmers that rely on manual harvesting practices (Adeleke et al., 2017; Kumar et al., 2020). Recent research shows the most effective solutions for reducing agricultural residue burning and its associated air pollution, are to encourage residue use for other purposes e.g., bioenergy, livestock feed/bedding, composting, green harvesting etc. (Kumar et al., 2020) and to apply coherent policies across multiple provinces and countries in Southeast Asia (Moran et al., 2019).

Discussion of the implementation and benefits of policies addressing deforestation and/or savanna-type fires in Southeast Asia are lacking in the literature. However, a number of policies and projects have been developed and implemented to address forest loss and conversion, many of which are related to UNFCCC REDD+ (reducing emissions from deforestation and forest degradation and the role of conservation, sustainable management of forest and enhancement of forest carbon stocks) (e.g., Kissinger, 2020). Key drivers of deforestation are expansion of cropland and commercial agriculture (Lim et al., 2017; Y. Zhang et al., 2018) e.g., conversion of forest to coffee and/or rubber plantations (Fox & Castella, 2013; Kissinger, 2020). There is evidence that protected areas and community-protected forests can play an important role in protecting forests from large-scale burning and deforestation fires (Biswas et al., 2015; Singh et al., 2018).

5 Conclusions

In this study we explored the impact of forest and vegetation fires on air quality and public health across Southeast Asia. We used a combination of two air quality models: a global aerosol model, GLOMAP, to test three different satellite-derived fire emission datasets (FINN, GFED, GFAS); and a high-resolution, regional air quality model, WRF-Chem, to quantify the air quality and public health benefits of eliminating fire emissions. Simulating the elimination of all fires across the region, rather than fires specifically identified to be human-caused, illustrates the maximum possible public health benefit achievable (within uncertainties) and provides an upper bound for policy makers.

We found that GLOMAP was better able to reproduce measurements of fire-derived PM in Thailand across multiple years with the FINN dataset compared to the GFAS or GFED datasets. This result is consistent with findings in our previous work (Reddington et al., 2016). PM emissions across Southeast Asia in FINN are a factor 4 greater than GFED or GFAS. WRF-Chem using FINN best simulated measured PM concentrations when particulate fire emissions were scaled upwards by a factor 1.5. Our analysis suggests fire emissions in this region are underestimated, particularly in the GFED and GFAS datasets.

Overall, we found that preventing fire could substantially improve regional air quality in Mainland Southeast Asia with a more limited benefit to air quality in south-eastern China. Population-weighted annual mean $PM_{2.5}$ concentrations were reduced by 16% in Mainland Southeast Asia and by 2% in south-eastern China. ADM8h O_3 concentrations were reduced by 9% in Mainland Southeast Asia and by 2% in south-eastern China. Eliminating fire emissions substantially reduced populations exposed to $PM_{2.5}$ concentrations above WHO AQ Interim Target 2 in Thailand, Myanmar, Laos and Cambodia (by 44-100%).

We found a considerable public health benefit of eliminating fire emissions across the region, largely due to reductions in $PM_{2.5}$ exposures. The annual disease burden due to $PM_{2.5}$ exposure was reduced by 12% in Mainland Southeast Asia, averting 27,500 (95UI: 24,700-30,400) premature deaths, and by 3% in south-eastern China, averting 31,400 (95UI: 30,500-32,400) premature deaths. The annual disease burden due to O_3 exposure was reduced by 10% in Mainland Southeast Asia, averting 2,250 (95UI: 2,000-2,470) premature deaths, and by 1% in south-eastern China, averting 1,530 (95UI: 1,380-1,660) premature deaths.

Using subnational poverty-proxy data, we found that poorer populations in Southeast Asia are disproportionally exposed to $PM_{2.5}$ from vegetation and forest fires; with significantly higher average fire-derived $PM_{2.5}$ exposure for populations with relatively high infant mortality rates.

Our analysis suggests that exposure to fire-derived $PM_{2.5}$ is associated with a greater annual disease burden in Southeast Asia than in both the Amazon region in 2012 and Equatorial Asia in 2015, with similar per capita averted disease burdens to those estimated for heavily fire-impacted countries in South America. Furthermore, preventing fires across Mainland Southeast Asia would yield a public health benefit comparable to that achieved by eliminating all industrial emissions across the region, and considerably larger than achieved by eliminating emissions from either the electricity generation or land transport sectors.

In summary, forest and vegetation fires are important to consider in addition to more traditional emission sectors (e.g., industry, transport and residential solid-fuel combustion) when assessing causes of air quality degradation in Southeast Asia and for developing emission control policies to improve air quality across this region. These policies should focus on reducing deforestation and savanna type fires in addition to agricultural fires in order to effectively address the regional air quality issues. Previous work in Equatorial Asia (Reddington et al., 2014) demonstrates the need to understand the effectiveness of regional emission control strategies and how they will reduce population exposure. Future work is required to identify the regions where emission controls would most effectively reduce exposure, especially for the poorest populations.

Contributions

CLR and DVS designed the research. CLR performed all model simulations, conducted the data analysis, and wrote the manuscript. LC conducted the public health impact calculations. SR processed the PCD measurement data. CK provided WRFotron, a tool to automatize WRF-Chem runs with re-initialised meteorology. SR, DVS and LC contributed to scientific discussions and to the manuscript.

Data availability

The air pollution and health impact assessment data per country/region that support the findings of this study are available at the Research Data Leeds Repository (https://doi.org/10.5518/968). Code to setup and run WRFChem (using WRFotron version 2.0) is available through Conibear and Knote (2020).

Acknowledgements

We gratefully acknowledge support from the AIA Group Limited and the Natural Environment Research Council (NE/S006680/1). This work was undertaken on Advanced Research Computing, part of the High Performance Computing facilities at the University of Leeds, UK. This work used WRFotron version 2.0, a tool to automatise WRFChem runs with re-initialised meteorology (Conibear & Knote, 2020). We acknowledge the use of WRFChem preprocessor tools mozbc, fire_emiss, anthro_emiss, bio_emiss provided by the Atmospheric Chemistry Observations and Modeling Laboratory of the National Center for Atmospheric Research. We acknowledge the use of Model for Ozone and Related Chemical Tracers version 4 (MOZART-4) global model output available at https://www.acom.ucar.edu/wrf-chem/mozart.shtml. We declare no competing financial interests. The boundaries shown on any maps in this work do not imply any judgement concerning the legal status of any territory or the endorsement or acceptance of such boundaries.

References

Adeleke, A., Apidechkul, T., Kanthawee, P., Suma, Y., and Wongnuch, P. (2017). Contributing factors and impacts of open burning in Thailand: perspectives from farmers in Chiang Rai province, Thailand, *Journal of Health Research*, 31(2), 159-67, doi:10.14456/jhr.2017.20

Adetona, O., Reinhardt, T. E., Domitrovich, J., Broyles, G., Adetona, A. M., Kleinman, M. T., et al. (2016). Review of the health effects of wildland fire smoke on wildland firefighters and the public, *Inhalation Toxicology*, 28(3), 95–139. https://doi.org/10.3109/08958378.2016.1145771

Adrianto, H.A., Spracklen, D.V., and Arnold, S.R. (2019). Relationship Between Fire and Forest Cover Loss in Riau Province, Indonesia Between 2001 and 2012, *Forests*, 10, 889, https://doi.org/10.3390/f10100889

Adrianto, H.A., Spracklen, D.V., Arnold, S.R., Sitanggang, I.S., and Syaufina, L. (2020). Forest and Land Fires Are Mainly Associated with Deforestation in Riau Province, Indonesia. *Remote Sensing*, *12*, 3. https://doi.org/10.3390/rs12010003

Aguilera, R., Corringham, T., Gershunov, A. et al. (2021). Wildfire smoke impacts respiratory health more than fine particles from other sources: observational evidence from Southern California. *Nature Communications*, 12, 1493. https://doi.org/10.1038/s41467-021-21708-0

Arnold, S. R., Chipperfield, M. P., and Blitz, M. A. (2005). A three dimensional model study of the effect of new temperature dependent quantum yields for acetone photolysis, *Journal of Geophysical Research*, 110, D22305, doi:10.1029/2005JD005998

Balk, D., G. D. Deane, M. A. Levy, A. Storeygard, and S. Ahamed (2006). The Biophysical Determinants of Global Poverty: Insights from an Analysis of Spatially Explicit Data. Paper presented at the 2006 Annual Meeting of the Population Association of America, Los Angeles, CA, 30 March-1 April 2006.

Barbier, E.B., and Hochard, J.P. (2018). Land degradation and poverty. *Nature Sustainability*, 1, 623–631, https://doi.org/10.1038/s41893-018-0155-4

Barbier, E.B., and Hochard, J.P. (2019). Poverty-Environment Traps. *Environmental and Resource Economics*, 74, 1239–1271, https://doi.org/10.1007/s10640-019-00366-3

Barlow, M., Zaitchik, B., Paz, S., Black, E., Evans, J., and Hoell, A. (2016). A Review of Drought in the Middle East and Southwest Asia, *Journal of Climate*, *29*(23), 8547-8574, https://journals.ametsoc.org/view/journals/clim/29/23/jcli-d-13-00692.1.xml

Biswas, S., Vadrevu, K. P., Lwin, Z. M., Lasko, K., and Justice, C. O. (2015). Factors controlling vegetation fires in protected and non-protected areas of Myanmar, *PLoS ONE*, 10, e0124346, https://doi.org/10.1371/journal.pone.0124346

Burnett, R., Chen, H., Szyszkowicz, M., Fann, N., Hubbell, B., Pope Iii, C.A., Apte, J.S., Brauer, M., Cohen, A., Weichenthal, S., Coggins, J., Di, Q., Brunekreef, B., Frostad, J., Lim, S.S., Kan, H., Walker, K.D., Thurston, G.D., Hayes, R.B., Lim, C.C., Turner, M.C., Jerrett, M., Krewski, D., Gapstur, S.M., Diver, W.R., Ostro, B., Goldberg, D., Crouse, D.L., Martin, R.V., Peters, P., Pinault, L., Tjepkema, M., van Donkelaar, A., Villeneuve, P.J., Miller, A.B., Yin, P., Zhou, M., Wang, L., Janssen, N.A.H., Marra, M., Atkinson, R.W., Tsang, H., Quoc Thach, T., Cannon, J.B., Allen, R.T., Hart, J.E., Laden, F., Cesaroni, G., Forastiere, F., Weinmayr, G., Jaensch, A., Nagel, G., Concin, H., and Spadaro, JV. (2018). Global estimates of mortality associated with longterm exposure to outdoor fine particulate matter, *Proceedings of the National Academy of Sciences*, 115 (38), 9592-9597, doi: 10.1073/pnas.1803222115, http://www.pnas.org/content/pnas/115/38/9592.full.pdf

Bruni Zani, N., Lonati, G., Mead, M. I., Latif, M. T., and Crippa, P. (2020). Long-term satellite-based estimates of air quality and premature mortality in Equatorial Asia through deep neural networks. *Environment Research Letters*, 15, 104088, https://doi.org/10.1088/1748-9326/abb733

Butt, E.W. et al. (2020). Large air quality and human health impacts due to Amazon forest and vegetation fires, *Environmental Research Communications*, 2, 095001, https://doi.org/10.1088/2515-7620/abb0db

Center for International Earth Science Information Network (CIESIN) (2016a). Columbia University. Gridded Population of the World, Version 4 (GPWv4): Population Count. Palisades, NY: NASA Socioeconomic Data and Applications Center (SEDAC). https://doi.org/10.7927/H4X63JVC

Center for International Earth Science Information Network (CIESIN) (2016b). Columbia University. Gridded Population of the World, Version 4 (GPWv4): Land and Water Area. Palisades, NY: NASA Socioeconomic Data and Applications Center (SEDAC). https://doi.org/10.7927/H45M63M9

Center for International Earth Science Information Network (CIESIN) (2018a). Columbia University. Global Subnational Infant Mortality Rates, Version 2. Palisades, NY: NASA Socioeconomic Data and Applications Center (SEDAC). https://doi.org/10.7927/H4PN93JJ. Accessed: 2 November 2020.

Center for International Earth Science Information Network (CIESIN) (2018b). Columbia University. Documentation for the Global Subnational Infant Mortality Rates, Version 2. Palisades, NY: NASA Socioeconomic Data and Applications Center (SEDAC). https://doi.org/10.7927/H44J0C25

Chan, L. Y., Chan, C. Y., Liu, H. Y., Christopher, S., Olt-mans, S. J., and Harris, J. M. (2000). A case study on the biomassburning in southeast Asia and enhancement of tropospherericozone over Hong Kong, *Geophysical Research Letters*, 27, 1479–1482, doi:10.1029/1999GL010855

Chan, C. Y., Chan, L. Y., Harris, J. M., Oltmans, S. J., Blake, D. R., Qin, Y., Zheng, Y. G., and Zheng, X. D. (2003). Characteristics of biomass burning emission sources, transport, and chemical speciation in enhanced springtime tropospheric ozone profile over Hong Kong, *Journal of Geophysical Research*, 108(D1), 4015, doi:10.1029/2001JD001555

Chen, J., Li, C., Ristovski, Z., Milic, A., Gu, Y., Islam, M. S., Wang, S., Hao, J., Zhang, H., He, C., Guo, H., Fu, H., Miljevic, B., Morawska, L., Thai, P., Lam, Y. F., Pereira, G., Ding, A., Huang, X., and Dumka, U. C. (2017). A review of biomass burning: emissions and impacts on air quality, health and climate in China, *Science of the Total Environment*, 579, 1000-1034, 10.1016/j.scitotenv.2016.11.025

Chipperfield, M. P. (2006). New version of the TOMCAT/SLIMCAT offline chemical transport model: Intercomparison of stratospheric tracer experiments, *Quarterly Journal of the Royal Meteorological Society*, 132, 1179–1203.

Conibear, L., and Knote, C. (2020). wrfchem-leeds/WRFotron: WRFotron 2.0. Zenodo. https://doi.org/http://doi.org/10.5281/zenodo.3624087

Conibear, L., Butt, E. W., Knote, C., Spracklen, D. V., and Arnold, S. R. (2018). Current and future disease burden from ambient ozone exposure in India, *GeoHealth*, 2, 334– 355. https://doi.org/10.1029/2018GH000168

Crippa, P., Castruccio, S., Archer-Nicholls, S., Lebron, G. B., Kuwata, M., Thota, A., et al. (2016). Population exposure to hazardous air quality due to the 2015 fires in Equatorial Asia, *Scientific Reports*, 6, 37074. https://doi.org/10.1038/srep37074

Dasgupta, P: An Inquiry into Well-Being and Destitution. Clarendon Press, Oxford, 1993.

Dasgupta, S., Deichmann, U., Meisner, C. and Wheeler, D. (2005). Where is the poverty–environment nexus? Evidence from Cambodia, Lao PDR, and Vietnam, *World Development*, 33, 617–638, https://doi.org/10.1016/j.worlddev.2004.10.003

de Oliveira Alves, N., Vessoni, A. T., Quinet, A., Fortunato, R. S., Kajitani, G. S., Peixoto, M. S., Hacon, S. D., Artaxo, P., Saldiva, P., Menck, C. F. M., and Batistuzzo de Medeiros, S. R. (2017). Biomass burning in the Amazon region causes DNA damage and cell death in human lung cells, *Scientific Reports*, 7, 10937, https://doi.org/10.1038/s41598-017-11024-3

De Sherbinin, A. (2008). Is poverty more acute near parks? An assessment of infant mortality rates around protected areas in developing countries. *Oryx, 42*(1), 26-35. doi:10.1017/S0030605308000781

Dee, D.P., Uppala, S.M., Simmons, A.J., Berrisford, P., Poli, P., Kobayashi, S., Andrae, U., Balmaseda, M.A., Balsamo, G., Bauer, P., Bechtold, P., Beljaars, A.C.M., van de Berg, L., Bidlot, J., Bormann, N., Delsol, C., Dragani, R., Fuentes, M., Geer, A.J., Haimberger, L., Healy, S.B., Hersbach, H., Hólm, E.V., Isaksen, L., Kållberg, P., Köhler, M., Matricardi, M., McNally, A.P., Monge-Sanz, B.M., Morcrette, J.-J., Park, B.-K., Peubey, C., de Rosnay, P., Tavolato, C., Thépaut, J.-N. and Vitart, F. (2011), The ERA-Interim reanalysis: configuration and performance of the data assimilation system, *Quarterly Journal of the Royal Meteorological Society*, 137: 553-597. https://doi.org/10.1002/qj.828

Deng, X., Tie, X. Zhou, X., Wu, D., Zhong, L., Tan, H., Li, F., et al. (2008). Effects of Southeast Asia biomass burning on aerosols and ozone concentrations over the Pearl River Delta (PRD) region, *Atmosperic Environment*, 42 (36), 8493-8501

Dentener, F., Kinne, S., Bond, T., Boucher, O., Cofala, J., Generoso,S., Ginoux, P., Gong, S., Hoelzemann, J. J., Ito, A., Marelli, L.,Penner, J. E., Putaud, J.-P., Textor, C., Schulz, M., van der Werf,G. R., and Wilson, J. (2006). Emissions of primary aerosol and precur-sor gases in the years 2000 and 1750 prescribed data-sets for Ae-roCom, *Atmospheric Chemistry and Physics*, 6, 4321–4344, doi:10.5194/acp-6-4321-2006

Duc, H.N., Bang, H.Q., and Quang, N.X. (2016). Modelling and prediction of air pollutant transport during the 2014 biomass burning and forest fires in peninsular Southeast Asia, *Environmental Monitoring and Assessment*, 188, 106, https://doi.org/10.1007/s10661-016-5106-9

Emmons, L. K., Walters, S., Hess, P. G., Lamarque, J.-F., Pfister, G. G., Fillmore, D., Granier, C., Guenther, A., Kinnison, D., Laepple, T., Orlando, J., Tie, X., Tyndall, G., Wiedinmyer, C., Baughcum, S. L., and Kloster, S. (2010). Description and evaluation of the Model for Ozone and Related chemical Tracers, version 4 (MOZART-4), *Geoscientific Model Development*, 3, 43-67, https://doi.org/10.5194/gmd-3-43-2010

Fairburn, J., Schüle, S.A., Dreger, S., Karla Hilz, L., and Bolte, G. (2019). Social Inequalities in Exposure to Ambient Air Pollution: A Systematic Review in the WHO European Region.

International Journal of Environmental Research and Public Health, 16, 3127, https://doi.org/10.3390/ijerph16173127

Fox, J., and Castella, J.C. (2013). Expansion of rubber (Hevea brasiliensis) in Mainland Southeast Asia: what are the prospects for smallholders?, *Journal of Peasant Studies*, 40(1), 155–170, https://doi.org/10.1080/03066150.2012.750605

Freitas, S. R., Longo, K. M., Chatfield, R., Latham, D., Silva Dias, M. A. F., Andreae, M. O., Prins, E., Santos, J. C., Gielow, R., and Carvalho Jr., J. A. (2007). Including the sub-grid scale plume rise of vegetation fires in low resolution atmospheric transport models, *Atmospheric Chemistry and Physics*, 7, 3385–3398, https://doi.org/10.5194/acp-7-3385-2007

Fritzell, J., Rehnberg, J., Bacchus Hertzman, J. and Blomgren, J. (2015). Absolute or relative? A comparative analysis between poverty and mortality. *International Journal of Public Health*, 60, 101–110, doi:10.1007/s00038-014-0614-2

Fu, J. S., Hsu, N. C., Gao, Y., Huang, K., Li, C., Lin, N.-H., and Tsay, S.-C. (2012). Evaluating the influences of biomass burning during 2006 BASE-ASIA: a regional chemical transport modeling, *Atmospheric Chemistry and Physics*, 12, 3837–3855, https://doi.org/10.5194/acp-12-3837-2012

Gautam, R., Hsu, N.C., Eck, T.F., Holben, B.N., Janjai, S., Jantarach, T., Tsay, S.-C., and Lau, W.K. (2013). Characterization of aerosols over the Indochina peninsula from satellite-surface observations during biomass burning pre-monsoon season, *Atmospheric Environment*, 78, 51-59, https://doi.org/10.1016/j.atmosenv.2012.05.038

GBD (Global Burden of Disease) 2015 Risk Factors Collaborators (2016). Global, regional, and national comparative risk assessment of 79 behavioural, environmental and occupational, and metabolic risks or clusters of risks, 1990-2015: a systematic analysis for the Global Burden of Disease Study 2015, *Lancet*, 388, 1659–1724, https://doi.org/10.1016/S0140-6736(16)31679-8

GBD (Global Burden of Disease) 2017 Risk Factors Collaborators (2018). Global, regional, and national comparative risk assessment of 84 behavioural, environmental and occupational, and metabolic risks or clusters of risks for 195 countries and territories, 1990–2017: a systematic analysis for the Global Burden of Disease Study 2017, *Lancet*, 392, 1923–1994, https://doi.org/10.1016/S0140-6736(18)32225-6

Giani, P., Anav, A., De Marco, A., Zhaozhong, F. and Crippa, P. (2020). Exploring sources of uncertainty in premature mortality estimates from fine particulate matter: the case of China**,** *Environment Research Letters*, 15, 064027, https://doi.org/10.1088/1748-9326/ab7f0f

Granier, C., Bessagnet, B., Bond, T., D'Angiola, A., Denier van der Gon, H., Frost, G. J., Heil, A., Kaiser, J. W., Kinne, S., Klimont,Z., Kloster, S., Lamarque, J.-F., Liousse, C., Masui, T., Meleux, F., Mieville, A., Ohara, T., Raut, J.-C., Riahi, K., Schultz, M.G., Smith, S. J., Thompson, A., Aardenne, J., van der Werf, G.R., and Vuuren, D. P. (2011). Evolution of anthropogenic and biomass burning emissions of air pollutants at global and regional scales during the 1980–2010 period, *Climatic Change*, 109, 163–190, https://doi.org/10.1007/s10584-011-0154-1

Grell, G. A., Peckham, S.E., Schmitz, R. McKeen, S. A., Frost, G., Skamarock, W. C., and Edere, B. (2005). Fully coupled 'online' chemistry within the WRF model, *Atmospheric Environment*, 39, 6957-6975, https://doi.org/10.1016/j.atmosenv.2005.04.027

Guenther, A., Hewitt, C. N., Erickson, D., Fall, R., Geron, C., Graedel, T., Harley, P., Klinger, L., Lerdau, M., McKay, W. A.,Pierce, T., Scholes, B., Steinbrecher, R., Tallamraju, R., Taylor, J., and Zimmerman, P. (1995). A global model of natural volatile organic compound emissions, *Journal of Geophysical Research*, 100, 8873–8892.

Guenther, A., Karl, T., Harley, P., Wiedinmyer, C., Palmer, P. I., and Geron, C. (2006). Estimates of global terrestrial isoprene emissions using MEGAN (Model of Emissions of Gases and Aerosols from Nature), *Atmospheric Chemistry and Physics*, 6, 3181-3210, https://doi.org/10.5194/acp-6-3181-2006

Hajat, A., Hsia, C., and O'Neill, M. S. (2015). Socioeconomic Disparities and Air Pollution Exposure: a Global Review, *Current Environmental Health Reports*, 2(4), 440–450. https://doi.org/10.1007/s40572-015-0069-5

Hauenstein, S., Kshatriya, M., Blanc, J. et al. (2019). African elephant poaching rates correlate with local poverty, national corruption and global ivory price. *Nature Communications,* 10, 2242. https://doi.org/10.1038/s41467-019-09993-2

Hijmans, R. (2016). University of California, Berkeley Museum of Vertebrate Zoology, Kapoor, J., Wieczorek, J., International Rice Research Institute, et al.: Global Administrative Areas (GADM): Boundaries without limits. Version 2.8.

Hodzic, A. and Jimenez, J. L. (2011). Modeling anthropogenically controlled secondary organic aerosols in a megacity: a simplified framework for global and climate models, *Geoscientific Model Development*, 4, 901-917.

Hodzic, A. and Knote, C. (2014). WRF-Chem 3.6.1: MOZART gas-phase chemistry with MOSAIC aerosols, Atmospheric Chemistry Division (ACD), National Center for Atmospheric Research (NCAR).

Huang, K., Fu, J. S., Hsu, N. C., Gao, Y., Dong, X., Tsay, S.-C., and Lam, Y. F. (2013). Impact assessment of biomass burning on air quality in Southeast and East Asia during BASE-ASIA, *Atmospheric Environment*, 78, 291-302, https://doi.org/10.1016/j.atmosenv.2012.03.048

Huang, W.-R., Wang, S.-H., Yen, M.-C., Lin, N.-H., and Promchote, P. (2016). Interannual variation of springtime biomass burning in Indochina: Regional differences, associated atmospheric dynamical changes, and downwind impacts, *Journal of Geophysical Research: Atmospheres*, 121, 10,016-10,028, doi:10.1002/2016JD025286

Institute for Health Metrics and Evaluation (2019). Global Burden of Disease (GBD) Compare Data Visualization. Retrieved February 13, 2019, from https://vizhub.healthdata.org/gbd-compare/

Jacobson, L. D. S. V., Hacon, S. D. S., Castro, H. A. D., Ignotti, E., Artaxo, P., Saldiva, P. H. N., and Leon, A. C. M. P. D. (2014). Acute effects of particulate matter and black carbon from seasonal fires on peak expiratory flow of schoolchildren in the Brazilian Amazon, *PLoS ONE*, 9, e104177, https://doi.org/10.1371/journal.pone.0104177

Jaffe, D. A. and Wigder, N. L. (2012). Ozone production from wildfires: A critical review, *Atmosperic Environment*, 51, 1–10, https://doi.org/10.1016/j.atmosenv.2011.11.063

Janjai, S., Suntaropas, S., and Nunez, M. (2009). Investigation of aerosol optical properties in Bangkok and suburbs, *Theoretical and Applied Climatology*, 96, 221-233, https://doi.org/10.1007/s00704-008-0026-4

Janssens-Maenhout, G., Crippa, M., Guizzardi, D., Dentener, F., Muntean, M., Pouliot, G., Keating, T., Zhang, Q., Kurokawa, J., Wankmüller, R., Denier van der Gon, H., Kuenen, J. J. P., Klimont, Z., Frost, G., Darras, S., Koffi, B., and Li, M. (2015). HTAP_v2.2: a mosaic of regional and global emission grid maps for 2008 and 2010 to study hemispheric transport of air pollution, *Atmospheric Chemistry and Physics*, 15, 11411-11432, https://doi.org/10.5194/acp-15-11411-2015

Jayachandran, S. (2009). Air quality and early-life mortality evidence from Indonesia's wildfires, *Journal of Human Resources*, 44, 916–54, doi:10.3386/w14011

Johnston, F. H., Henderson, S. B., Chen, Y., Randerson, J. T., Marlier, M., Defries, R. S., Kinney, P., Bowman, D. M., and Brauer, M. (2012). Estimated global mortality attributable to smoke from landscape fires. *Environmental Health Perspectives*, *120*(5), 695–701. https://doi.org/10.1289/ehp.1104422

Johnston, H.J., Mueller, W., Steinle, S. et al. (2019). How Harmful Is Particulate Matter Emitted from Biomass Burning? A Thailand Perspective, *Current Pollution Reports*, 5, 353–377, https://doi.org/10.1007/s40726-019-00125-4

Kaiser, J. W., Heil, A., Andreae, M. O., Benedetti, A., Chubarova, N., Jones, L., Morcrette, J.-J., Razinger, M., Schultz, M. G., Suttie, M., and van der Werf, G. R. (2012). Biomass burning emissions estimated with a global fire assimilation system based on observations of fire radiative power, *Biogeosciences*, 9, 527-554, doi:10.5194/bg-9-527-2012

Kiely, L., et al. (2020). Air quality and health impacts of vegetation and peatfires in Equatorial Asia during 2004-2015, *Environment Research Letters*, 15, 094054, https://iopscience.iop.org/article/10.1088/1748-9326/ab9a6c

Kim Oanh, N. T., and Leelasakultum, K. (2011). Analysis of meteorology and emission in haze episode prevalence over mountain-bounded region for early warming, *Science of the Total Environment*, 409, 2261–2271, https://doi.org/10.1016/j.scitotenv.2011.02.022

Kissinger, G. (2020). Policy Responses to Direct and Underlying Drivers of Deforestation: Examining Rubber and Coffee in the Central Highlands of Vietnam, *Forests*, 11, 733, https://doi.org/10.3390/f11070733

Knote, C., Hodzic, A., Jimenez, J. L., Volkamer, R., Orlando, J. J., Baidar, S., Brioude, J., Fast, J., Gentner, D. R., Goldstein, A. H., Hayes, P. L., Knighton, W. B., Oetjen, H., Setyan, A., Stark, H., Thalman, R., Tyndall, G., Washenfelder, R., Waxman, E., and Zhang, Q. (2014). Simulation of semi-explicit mechanisms of SOA formation from glyoxal in aerosol in a 3-D model, *Atmospheric Chemistry and Physics*, 14, 6213-6239, https://doi.org/10.5194/acp-14-6213-2014

Kondo, Y., et al. (2004). Impacts of biomass burning in Southeast Asia on ozone and reactive nitrogen over the western Pacific in spring, *Journal of Geophysical Research*, 109, D15S12, doi:10.1029/2003JD004203

Koplitz, S. N., Mickley, L. J., Marlier, M. E., Buonocore, J. J., Kim, P. S., Liu, T. J., Sulprizio, M. P., DeFries, R. S., Jacob, D. J., Schwartz, J., Pongsiri, M. and Myers, S. S. (2016). Public health impacts of the severe haze in Equatorial Asia in September-October 2015: demonstration of a new framework for informing fire management strategies to reduce downwind smoke exposure, *Environment Research Letters*, 11, 10, https://doi.org/10.1088/1748-9326/11/9/094023

Kumar, I., Bandaru, V., Yampracha, S., Sun, L., Fungtammasan, B. (2020). Limiting rice and sugarcane residue burning in Thailand: Current status, challenges and strategies, *Journal of Environmental Management*, 276, 111228, https://doi.org/10.1016/j.jenvman.2020.111228

Lasko, K., Vadrevu, K.P., Tran, V.T., Ellicott, E., Nguyen, T.T.N., Bui, H.Q., and Justice, C. (2017). Satellites may underestimate rice residue and associated burning emissions in Vietnam, *Environment Research Letters*, 12, 085006, https://doi.org/10.1088/1748-9326/aa751d

Lasko, K., Vadrevu, K.P., Nguyen, T.T.N. (2018). Analysis of air pollution over Hanoi, Vietnam using multi-satellite and MERRA reanalysis datasets, *PLoS ONE*, 13(5): e0196629. https://doi.org/10.1371/journal.pone.0196629

Lee, H.-H., Bar-Or, R. Z., and Wang, C. (2017). Biomass burning aerosols and the low-visibility events in Southeast Asia, *Atmospheric Chemistry and Physics*, 17, 965–980, https://doi.org/10.5194/acp-17-965-2017

Lee, H.-H., Iraqui, O., Gu, Y., Yim, S. H.-L., Chulakadabba, A., Tonks, A. Y.-M., Yang, Z., and Wang, C. (2018). Impacts of air pollutants from fire and non-fire emissions on the regional air quality in Southeast Asia, *Atmospheric Chemistry and Physics*, 18, 6141–6156, https://doi.org/10.5194/acp-18-6141-2018

LeGrand, S. L., Polashenski, C., Letcher, T. W., Creighton, G. A., Peckham, S. E., and Cetola, J. D. (2019). The AFWA dust emission scheme for the GOCART aerosol model in WRF-Chem v3.8.1, *Geoscientific Model Development*, 12, 131-166, https://doi.org/10.5194/gmd-12-131-2019

Li, J., Zhang, Y., Wang, Z., Sun, Y., Fu, P., Yang, Y., Huang, H., Li, J., Zhang, Q., Lin, C. and Lin, N.H. (2017). Regional Impact of Biomass Burning in Southeast Asia on Atmospheric Aerosols during the 2013 Seven South-East Asian Studies Project, *Aerosol and Air Quality Research*, 17, 2924-2941, https://doi.org/10.4209/aaqr.2016.09.0422

Lim, C. L., Prescott, G. W., Alban, J. D. T. D., Ziegler, A. D. and Webb, E. L. (2017). Untangling the proximate causes and underlying drivers of deforestation and forest degradation in Myanmar, *Conservation Biology*, 31, 1362–1372, doi:10.1111/cobi.12984

Lin, N. H., Tsay, S. C., Maring, H. B., Yen, M. C., Sheu, G. R., Wang, S. H., Chi, K. H., Chuang, M. T., Ou-Yang, C. F., Fu, J. S., Reid, J. S., Lee, C. Te, Wang, L. C., Wang, J. L., Hsu, C. N., Sayer, A. M., Holben, B. N., Chu, Y. C., Nguyen, X. A., Sopajaree, K., Chen, S. J., Cheng, M. T., Tsuang, B. J., Tsai, C. J., Peng, C. M., Schnell, R. C., Conway, T., Chang, C. T., Lin, K. S., Tsai, Y. I., Lee, W. J., Chang, S. C., Liu, J. J., Chiang, W. L., Huang, S. J., Lin, T. H., and Liu, G. R. (2013). An overview of regional experiments on biomass burning aerosols and related pollutants in Southeast Asia: From BASE-ASIA and the Dongsha Experiment to 7-SEAS, *Atmospheric Environment*, 78, 1–19, https://doi.org/10.1016/j.atmosenv.2013.04.066

Liu, J. C., Pereira, G., Uhl, S. A., Bravo, M. A., and Bell, M. L. (2015). A systematic review of the physical health impacts from non-occupational exposure to wildfire smoke. *Environmental Research*, 136, 120–132. https://doi.org/10.1016/j.envres.2014.10.015

Liu, T., Mickley, L. J., Marlier, M. E., DeFries, R. S., Khan, M. F., Latif, M. T., and Karambelas, A. (2020). Diagnosing spatial biases and uncertainties in global fire emissions inventories: Indonesia as regional case study, *Remote Sensing of Environment*, 237, 111557, https://doi.org/10.1016/j.rse.2019.111557

Mann, G. W., Carslaw, K. S., Spracklen, D. V., Ridley, D. A., Manktelow, P. T., Chipperfield, M. P., Pickering, S. J., and Johnson, C. E. (2010). Description and evaluation of GLOMAP-mode: a modal global aerosol microphysics model for the UKCA composition-climate model, *Geoscientific Model Development*, 3, 519-551, doi:10.5194/gmd-3-519-2010

Marlier, M. E., Defries, R. S., Voulgarakis, A., Kinney, P. L., Randerson, J. T., Shindell, D. T., Chen, Y., and Faluvegi, G. (2012). El Niño and health risks from landscape fire emissions in southeast Asia, *Nature Climate Change*, 3, 131–6, https://www.nature.com/articles/nclimate1658

Mehta, S, Sbihi, H., Dinh, T.N., Xuan, D.V., Le Thi Thanh, L., Thanh, C.T., et al. (2014). Effect of poverty on the relationship between personal exposures and ambient concentrations of air pollutants in Ho Chi Minh City, *Atmospheric Environment*, 95, 571-580, https://doi.org/10.1016/j.atmosenv.2014.07.011

Moran, J., NaSuwan, C., and Poocharoen, O.-O. (2019). The haze problem in northern Thailand and policies to combat it: a review, *Environmental Science & Policy*, 97, 1–15, https://doi.org/10.1016/j.envsci.2019.03.016

Mu, M., Randerson, J. T., van der Werf, G. R., Giglio, L, Kasibhatla, P., Morton, D., Collatz, G. J., DeFries, R. S., Hyer, E. J., Prins, E. M., Griffith, D. W. T., Wunch, D., Toon, G. C., Sherlock V., and Wennberg, P. O. (2011). Daily and 3-hourly variability in global fire emissions and consequences for atmospheric model predictions of carbon monoxide, *Journal of Geophysical Research*, 116, D24303, doi: 10.1029/2011JD016245

Myanmar Ministry of Health (2003). Report of overall and cause specific under five mortality survey (2002-03). Yangon: Department of Health.

Naeher, L. P., Brauer, M., Lipsett, M., Zelikoff, J. T., Simpson, C. D., Koenig, J. Q., et al. (2007). Woodsmoke Health Effects: A Review, *Inhalation Toxicology*, 19(1), 67–106. https://doi.org/10.1080/08958370600985875

Narloch, U., and Bangalore, M. (2018). The multifaceted relationship between environmental risks and poverty: New insights from Vietnam, *Environment and Development Economics, 23*(3), 298-327, doi:10.1017/S1355770X18000128

Nawaz, M. O., and Henze, D. K. (2020). Premature deaths in Brazil associated with long-term exposure to PM2.5 from Amazon fires between 2016-2019, *GeoHealth*, 4, e2020GH000268, https://doi.org/10.1029/2020GH000268

NCAR (National Center for Atmospheric Research) (2016). ACOM MOZART-4/GEOS-5 global model output, UCAR. Available at: http://www.acom.ucar.edu/wrf-chem/mozart.shtml.

NCEP (2000). National Weather Service, NOAA & U.S. Department of Commerce. NCEP Final (FNL) Operational Model Global Tropospheric Analyses, continuing from July 1999. Research Data Archive at the National Center for Atmospheric Research, Computational and Information Systems Laboratory, https://doi.org/10.5065/D6M043C6

NCEP (2007). National Weather Service, NOAA & U.S. Department of Commerce. NCEP Global Forecast System (GFS) Analyses and Forecasts. Research Data Archive at the National Center for Atmospheric Research, Computational and Information Systems Laboratory, http://rda.ucar.edu/datasets/ds084.6/

Nodzu, M.I., Ogino, S., Tachibana, Y., and Yamanaka, M. D. (2006). Climatological description of seasonal variations in lower tropospheric temperature inversions layers over the Indochina Peninsula, *Journal of Climate*, 19, 3307-3319, https://doi.org/10.1175/JCLI3792.1

Nguyen, T. T. N., Pham, H. V., Lasko, K., Bui, M. T., Laffly, D., Jourdan, A., and Bui, H. Q. (2019). Spatiotemporal analysis of ground and satellite-based aerosol for air quality assessment in the Southeast Asia region, *Environmental Pollution*, 255, 113106, https://doi.org/10.1016/j.envpol.2019.113106

O'Hare, B., Makuta, I., Chiwaula, L., and Bar-Zeev, N. (2013). Income and child mortality in developing countries: a systematic review and meta-analysis. *Journal of the Royal Society of Medicine*, *106*(10), 408–414. https://doi.org/10.1177/0141076813489680

Pan, X., Ichoku, C., Chin, M., Bian, H., Darmenov, A., Colarco, P., Ellison, L., Kucsera, T., da Silva, A., Wang, J., Oda, T., and Cui, G. (2020). Six global biomass burning emission datasets: intercomparison and application in one global aerosol model, *Atmospheric Chemistry and Physics*, 20, 969–994, https://doi.org/10.5194/acp-20-969-2020

Pasanen, T., Lakkala, H., Yliluoma, R., Tuominen,V., Jusi, S., Luukkanen, J., and Kaivo-oja, J. (2017). Poverty–environment nexus in the Lao PDR: Analysis of household survey data, *Development Policy Review*, 35(3), 349-371, https://doi.org/10.1111/dpr.12212

Pengchai, P., Chantara, S., Sopajaree, K., Wangkarn, S., Tencharoenkul, U., Rayanakorn, M. (2009). Seasonal variation, risk assessment and source estimation of PM10 and PM10-bound PAHs in the ambient air of Chiang Mai and Lamphun, Thailand. *Environmental Monitoring and Assessment*, 154, 197–218, doi:10.1007/s10661-008-0389-0

Phairuang, W., Hata, M., and Furuuchi, M. (2017). Influence of agricultural activities, forest fires and agro-industries on air quality in Thailand, *Journal of Environmental Sciences*, 52, 85–97, https://doi.org/10.1016/j.jes.2016.02.007.

Pienkowski, T., Dickens, B.L., Sun, H., and Carrasco, L.R. (2017). Empirical evidence of the public health benefits of tropical forest conservation in Cambodia: a generalised linear mixed-effects model analysis, *The Lancet Planetary Health*, 1: e180–87, https://doi.org/10.1016/S2542-5196(17)30081-5

Pimonsree, S., Vongruang, P., and Sumitsawan, S. (2018). Modified biomass burning emission in modeling system with fire radiative power: simulation of particulate matter in Mainland Southeast Asia during smog episode, *Atmospheric Pollution Research*, 9 (1), 133-145, http://doi.org/10.1016/j.apr.2017.08.002

Pochanart, P., Kreasuwun, J., Sukasem, P., Geeratithadaniyom, W., Tabucanon, M. S., Hirokawa, J., Kajii, Y., and Akimoto, H. (2001). Tropical tropospheric ozone observed in Thailand, *Atmospheric Environment*, 35, 2657–2668, https://doi.org/10.1016/S1352-2310(00)00441-6

Pongpiachan, S. (2016). Incremental lifetime cancer risk of PM2.5 bound polycyclic aromatic hydrocarbons (PAHs) before and after the Wildland fire episode, *Aerosol and Air Quality Research*, 16, 2907-2919, https://doi.org/10.4209/aaqr.2015.01.0011

Pongpiachan, S. and Paowa, T. (2015). Hospital out-and-in-patients as Functions of Trace Gaseous Species and Other Meteorological Parameters in Chiang-Mai, Thailand, *Aerosol and Air Quality Research*, 15, 479-493, https://doi.org/10.4209/aaqr.2013.09.0293.

Randerson, J. T., Chen, Y., van der Werf, G. R., Rogers, B. M., and Morton, D. C. (2012). Global burned area and biomass burningemissions from small fires, *Journal of Geophysical Research*, 117, G04012, doi:10.1029/2012JG002128

Reddington, C. L., Yoshioka, M., Balasubramanian, R., Ridley, D., Toh, Y. Y., Arnold, S. R., and Spracklen, D. V. (2014). Contribution of vegetation and peat fires to particulate air pollution in South-east Asia, *Environment Research Letters*, 9, 094006, doi:10.1088/1748-9326/9/9/094006

Reddington, C. L., Butt, E. W., Ridley, D. A., Artaxo, P., Morgan,W. T., Coe, H., and Spracklen, D. V. (2015). Air quality and human health improvements from reductions in deforestation-related fire in Brazil, *Nature Geoscience*, 8, 768–771, doi:10.1038/ngeo2535

Reddington, C. L., Spracklen, D. V., Artaxo, P., Ridley, D. A., Rizzo, L. V., and Arana, A. (2016). Analysis of particulate emissions from tropical biomass burning using a global aerosol model and long-term surface observations, *Atmospheric Chemistry and Physics*, 16, 11083–11106, https://doi.org/10.5194/acp-16-11083-2016

Reddington, C. L., Conibear, L., Knote, C., Silver, B. J., Li, Y. J., Chan, C. K., Arnold, S. R., and Spracklen, D. V. (2019a). Exploring the impacts of anthropogenic emission sectors on $PM_{2.5}$ and human health in South and East Asia, *Atmospheric Chemistry and Physics*, 19, 11887–11910, https://doi.org/10.5194/acp-19-11887-2019

Reddington, C. L., Morgan, W. T., Darbyshire, E., Brito, J., Coe, H., Artaxo, P., Scott, C. E., Marsham, J., and Spracklen, D. V. (2019b). Biomass burning aerosol over the Amazon: analysis of aircraft, surface and satellite observations using a global aerosol model, *Atmospheric Chemistry and Physics*, 19, 9125–9152, https://doi.org/10.5194/acp-19-9125-2019

Reid, C.E., Brauer, M., Johnston, F.H., Jerrett, M., Balmes, J.R. and Elliott, C.T. (2016) Critical review of health impacts of wildfire smoke exposure, *Environmental Health Perspectives*, 124 (9), 1334-1343, doi:10.1289/ehp.1409277

Reidpath, D.D., and Allotey, P. (2003). Infant mortality rate as an indicator of population health, *Journal of Epidemiology & Community Health*, 57, 344-346, doi:10.1136/jech.57.5.344

Rohde, R. A. and Muller, R. A. (2015). Air pollution in China: mapping of concentrations and sources, *PLoS ONE*, 10, 1-14, doi:10.1371/journal.pone.0135749

Sang, X.F., Zhang, Z.S., Chan, C.Y., and Engling, G. (2013). Source categories and contribution of biomass smoke to organic aerosol over the southeastern Tibetan Plateau, *Atmospheric Environment*, 78, 113-123, https://doi.org/10.1016/j.atmosenv.2012.12.012

Sartorius, B. K. D., and Sartorius, K. (2014). Global infant mortality trends and attributable determinants – an ecological study using data from 192 countries for the period 1990–2011. *Population Health Metrics*, 12, 29, https://doi.org/10.1186/s12963-014-0029-6

Scott, C. E., Rap, A., Spracklen, D. V., Forster, P. M., Carslaw, K. S., Mann, G. W., Pringle, K. J., Kivekäs, N., Kulmala, M., Lihavainen, H., and Tunved, P. (2014). The direct and indirect radiative effects of biogenic secondary organic aerosol, *Atmospheric Chemistry and Physics*, 14, 447-470, https://doi.org/10.5194/acp-14-447-2014

Shen, L., Jacob, D. J., Zhu, L., Zhang, Q., Zheng, B., Sulprizio, M. P., et al. (2019). The 2005–2016 trends of formaldehyde columns over China observed by satellites: Increasing anthropogenic emissions of volatile organic compounds and decreasing agricultural fire emissions, *Geophysical Research Letters*, 46, 4468-4475, https://doi.org/10.1029/2019GL082172

Shi, Y., and Yamaguchi, Y. (2014). A high-resolution and multi-year emissions inventory for biomass burning in Southeast Asia during 2001–2010, *Atmospheric Environment*, 98, 8-16, https://doi.org/10.1016/j.atmosenv.2014.08.050

Singh, M., Evans, D., Chevance, J. B., et al. (2018). Evaluating the ability of community-protected forests in Cambodia to prevent deforestation and degradation using temporal remote sensing data. *Ecology and Evolution*, 8, 10175– 10191. https://doi.org/10.1002/ece3.4492

Sornpoon, W., Bonnet, S., Kasemsap, P., Prasertsak, P., and Garivait, S. (2014). Estimation of Emissions from Sugarcane Field Burning in Thailand Using Bottom-Up Country-Specific Activity Data, *Atmosphere*, 5, 669-685, https://doi.org/10.3390/atmos5030669

Spracklen, D. V., Pringle, K. J., Carslaw, K. S., Chipperfield, M. P., and Mann, G. W. (2005). A global off-line model of size-resolved aerosol microphysics: I. Model development and prediction of aerosol properties, *Atmospheric Chemistry and Physics*, 5, 2227-2252, doi:10.5194/acp-5-2227-2005

Stavrakou, T., Müller, J. F., Bauwens, M., De Smedt, I., Lerot, C., van Roozendael, M., Coheur, P. F., Clerbaux, C., Boersma, K. F., van der A, R., and Song, Y. (2016). Substantial underestimation of post-harvest burning emissions in the North China plain revealed by multi-species space observations, *Scientific Reports*, 6, 32307. https://doi.org/10.1038/srep32307

Takami, K., Shimadera, H., Uranishi, K., and Kondo, A. (2020). Impacts of Biomass Burning Emission Inventories and Atmospheric Reanalyses on Simulated PM10 over Indochina, *Atmosphere*, 11(2), 160, https://www.mdpi.com/2073-4433/11/2/160

Tsai, Y.I., Soparajee, K., Chotruksa, A., Wu, H.C., and Kuo, S.C. (2013). Source indicators of biomass burning associated with inorganic salts and carboxylates in dry season ambient aerosol in Chiang Mai basin, Thailand, *Atmospheric Environment*, 78, 93–104, https://doi.org/10.1016/j.atmosenv.2012.09.040

Turner, M. C., Jerrett, M., Pope III, C. A., Krewski, D., Gapstur, S. M., Diver, R. W., et al. (2016). Long-Term Ozone Exposure and Mortality in a Large Prospective Study, *American Journal of Respiratory and Critical Care Medicine*, 193(10), 1134–1142. https://doi.org/10.1164/rccm.201508-1633OC

United Nations Inter-agency Group for Child Mortality Estimation (2020). Infant mortality rate estimates developed by the United Nations Inter-agency Group for Child Mortality Estimation (UNIGME). Available at www.childmortality.org. Accessed: 5 May 2021.

Vadrevu, K.P., Lasko, K., Giglio, L., Schroeder, W., Biswas, S. and Justice, C. (2019). Trends in Vegetation fires in South and Southeast Asian Countries, *Scientific Reports*, 9, 7422, https://doi.org/10.1038/s41598-019-43940-x

Vajanapoom, N., Kooncumchoo, P., and Thach, T.Q. (2020). Acute effects of air pollution on all-cause mortality: a natural experiment from haze control measures in Chiang Mai Province, Thailand, *PeerJ*, 8, e9207, doi:10.7717/peerj.9207

van der Werf, G. R., Randerson, J. T., Giglio, L., Collatz, G. J., Mu, M., Kasibhatla, P. S., Morton, D. C., DeFries, R. S., Jin, Y., and van Leeuwen, T. T. (2010). Global fire emissions and the contribution of deforestation, savanna, forest, agricultural, and peat fires (1997-2009), *Atmospheric Chemistry and Physics*, 10, 11707-11735, doi:10.5194/acp-10-11707-2010

van der Werf, G. R., Randerson, J. T., Giglio, L., van Leeuwen, T. T., Chen, Y., Rogers, B. M., Mu, M., van Marle, M. J. E., Morton, D. C., Collatz, G. J., Yokelson, R. J., and Kasibhatla, P. S. (2017). Global fire emissions estimates during 1997–2016, *Earth Syst. Sci. Data*, 9, 697-720, https://doi.org/10.5194/essd-9-697-2017

Vongruang, P., and Pimonsree, S. (2020). Biomass burning sources and their contributions to PM10 concentrations over countries in mainland Southeast Asia during a smog episode, *Atmospheric Environment*, https://doi.org/10.1016/j.atmosenv.2020.117414, 228, 117414

Vongruang, P., Wongwises, P., and Pimonsree, S. (2017) Assessment of fire emission inventories for simulating particulate matter in Upper Southeast Asia using WRF-CMAQ, *Atmospheric Pollution Research*, 8 (5), 921-929, http://doi.org/10.1016/j.apr.2017.03.004

Wegesser, T. C., Pinkerton, K. E., and Last, J. A. (2009). California wildfires of 2008: Coarse and fine particulate matter toxicity, *Environmental Health Perspectives*, 117(6), 893–897. https://doi.org/10.1289/ehp.0800166

Western Regional Air Partnership (WRAP) (2005). 2002 Fire Emission Inventory for the WRAP Region- Phase II, Project No. 178-6, http://www.wrapair.org/forums/fejf/tasks/FEJFtask7PhaseII.html

Wiedinmyer, C., Akagi, S. K., Yokelson, R. J., Emmons, L. K., Al-Saadi, J. A., Orlando, J. J., and Soja, A. J.: The Fire INventory from NCAR (FINN): a high resolution global model to estimate the emissions from open burning, *Geoscientific Model Development*, 4, 625-641, https://doi.org/10.5194/gmd-4-625-2011, 2011.

World Health Organization (WHO) (2006). Air quality guidelines for particulate matter, ozone, nitrogen dioxide and sulfur dioxide: Global update 2005. Summary of risk assessment. http://www.who.int/phe/health_topics/outdoorair/outdoorair_aqg/en/

World Health Organization (WHO) (2016). Ambient Air Pollution: A Global Assessment Of Exposure And Burden Of Disease, Vol. 121, World Health Organization, Geneva, 1–131.

World Health Organization (WHO) (2018). WHO Global Ambient Air Quality Database (update 2018) edition, Version 1.0, Geneva, World Health Organization, 2018. Available at: https://www.who.int/airpollution/data/cities/en/, last access: 1 August 2019.

Yadav, I.C., Linthoingambi Devi, N., Li, J., Syed, J.H., Zhang, G., and Watanabe, H. (2017) Biomass burning in Indo-China peninsula and its impacts on regional air quality and global climate change-a review, *Environmental Pollution*, 227, 414-427, 10.1016/j.envpol.2017.04.085

Yin, P., Brauer, M., Cohen, A., Burnett, R. T., Liu, J., Liu, Y., et al. (2017). Long-term fine particulate matter exposure and nonaccidental and cause-specific mortality in a large national cohort of Chinese men, *Environmental Health Perspectives*, *125*(11), 117002–117011. https://doi.org/10.1289/EHP1673

Yin, S., Wang, X.F., Zhang, X.R., Guo, M. Miura, M., and Xiao, Y. (2019). Influence of biomass burning on local air pollution in mainland Southeast Asia from 2001 to 2016, *Environmental Pollution*, 254, 112949, https://doi.org/10.1016/j.envpol.2019.07.117

Yu, S., Eder, B., Dennis, R., Chu, S.-H., and Schwartz, S. E. (2006). New unbiased symmetric metrics for evaluation of air quality models, *Atmospheric Science Letters*, 7, 26-34. doi:10.1002/asl.125

Zaveri, R. A., Easter, R. C., Fast, J. D. and Peters, L. K. (2008). Model for Simulating Aerosol Interactions and Chemistry (MOSAIC), *Journal of Geophysical Research: Atmospheres*, 113, D13204, doi:10.1029/2007JD008782, https://doi.org/10.1029/2007JD008782

Zhang, L., Liu, Y., and Hao, L. (2016). Contributions of open crop straw burning emissions to PM2.5 concentrations in China, *Environment Research Letters*, 11, 014014, https://doi.org/10.1088/1748-9326/11/1/014014

Zhang, Y., Prescott, G.W., Tay, R.E. et al. (2018). Dramatic cropland expansion in Myanmar following political reforms threatens biodiversity, *Scientific Reports*, 8, 16558, https://doi.org/10.1038/s41598-018-34974-8

Zhang, T., Wooster, M.J., De Jong, M.C., and Xu, W. (2018). How Well Does the 'Small Fire Boost' Methodology Used within the GFED4.1s Fire Emissions Database Represent the Timing, Location and Magnitude of Agricultural Burning?, *Remote Sensing*, *10*, 823, https://doi.org/10.3390/rs10060823

Zhang, T., de Jong, M. C., Wooster, M. J., Xu, W., and Wang, L. (2020). Trends in eastern China agricultural fire emissions derived from a combination of geostationary (Himawari) and polar (VIIRS) orbiter fire radiative power products, *Atmospheric Chemistry and Physics*, 20, 10687–10705, https://doi.org/10.5194/acp-20-10687-2020

Zhu, J., Xia, X., Che, H., Wang, J., Zhang, J., and Duan, Y. (2016). Study of aerosol optical properties at Kunming in southwest China and long-range transport of biomass burning aerosols from North Burma, *Atmospheric Research*, 169, 237–247, https://doi.org/10.1016/j.atmosres.2015.10.012

GeoHealth

Supporting Information for

Air Pollution from Forest and Vegetation Fires in Southeast Asia Disproportionately Impacts the Poor

Carly L. Reddington*[,1], Luke Conibear[1], Suzanne Robinson[1], Christoph Knote[2], Stephen R. Arnold[1], and Dominick V. Spracklen[1]

[1] Institute for Climate and Atmospheric Science, School of Earth and Environment, University of Leeds, Leeds, UK

[2] Faculty of Medicine, University of Augsburg, Germany

* Corresponding author: Carly Reddington (C.L.S.Reddington@leeds.ac.uk)

S1. Methods

S1.1 Description of the GLOMAP global aerosol model

The Global Model of Aerosol Processes (GLOMAP) (Spracklen et al., 2005; Mann et al., 2010) is an extension of the TOMCAT global 3-D offline chemical transport model (Chipperfield, 2006), resolving aerosol chemistry and microphysics. The GLOMAP aerosol model has a horizontal resolution of 2.8°×2.8° with 31 vertical model levels between the surface and 10 hPa. Large-scale atmospheric transport and meteorology in are specified from European Centre for Medium-Range Weather Forecasting (ECMWF) ERA-Interim global reanalysis data (Dee et al., 2011), updated every six hours and linearly interpolated onto the model time step. The aerosol size distribution is represented by a two-moment modal aerosol scheme (Mann et al., 2010). GLOMAP includes black carbon (BC), primary and secondary organic aerosol, sulfate (SO_4), sea spray and mineral dust. Concentrations of oxidants are specified using monthly mean 3-D fields at 6-hourly intervals from a TOMCAT simulation with detailed tropospheric chemistry (Arnold et al., 2005) linearly interpolated onto the model time step.

Anthropogenic emissions of sulfur dioxide (SO_2), BC and organic carbon (OC) were specified using annually varying MACCity emissions inventory for the years 2002-2010 (Granier et al., 2011). For simulations in 2011 and beyond, we used MACCity anthropogenic emissions from 2010. Monthly mean emissions of biogenic monoterpenes are taken from the Global Emissions InitiAtive (GEIA) database (Guenther et al., 1995). Monoterpenes are oxidised to form a product that condenses irreversibly in the particle phase to form secondary organic aerosol (Scott et al., 2014). Size-resolved emissions of mineral dust are prescribed from daily varying emissions fluxes provided for AEROCOM (Dentener et al., 2006).

S1.2 Description of the WRF-Chem regional model

In the version of WRF-Chem used in this study, aerosol physics and chemistry are treated using the Model for Simulating Aerosol Interactions and Chemistry (MOSAIC; Zaveri et al., 2008) scheme, using chemistry option 201, with an extended treatment of organic aerosol (Hodzic and Jimenez, 2011; Hodzic and Knote, 2014). The MOSAIC scheme treats major aerosol species including SO_4, nitrate, chloride, ammonium, sodium, BC, primary and secondary organic aerosol (formed from biogenic, anthropogenic and biomass burning precursors), and other inorganics (including crustal and dust particles and residual primary $PM_{2.5}$). Four discrete size bins are used within MOSAIC to represent the aerosol size distribution (with the following dry particle diameter ranges: 0.039–0.156 µm, 0.156–0.625 µm, 0.625–2.5 µm, and 2.5–10 µm). Gas-phase chemical reactions are calculated using the extended Model for Ozone and Related Chemical Tracers (MOZART) (Emmons et al., 2010) chemical mechanism, with several updates to photochemistry of aromatics, biogenic hydrocarbons and other species relevant to regional air quality (Hodzic and Jimenez, 2011; Knote et al., 2014).

Simulated mesoscale meteorology is kept in line with analysed meteorology through grid nudging to the National Centre for Environmental Prediction (NCEP) Global Forecast System (GFS) analyses to limit errors in mesoscale transport (NCEP, 2000; 2007). The model meteorology was reinitialised every month to avoid drifting of WRF-Chem and spun up for 12 hours, while chemistry and aerosol fields were retained to allow for pollution build-up and mesoscale pollutant transport phenomena to be captured. MOZART-4/Goddard Earth Observing System Model version 5 (GEOS5) 6-hourly simulation data (NCAR, 2016) were used for chemical and aerosol boundary conditions.

Anthropogenic emissions were taken from the Emission Database for Global Atmospheric Research with Task Force on Hemispheric Transport of Air Pollution (EDGAR-HTAP) version 2.2 at 0.1°×0.1° horizontal resolution (Janssens-Maenhout et al., 2015). Biogenic emissions were calculated online by the Model of Emissions of Gases and Aerosol from Nature (MEGAN; Guenther et al., 2006). Dust emissions were calculated online through the Georgia Institute of Technology-Goddard Global Ozone Chemistry Aerosol Radiation and Transport (GOCART) model with Air Force Weather Agency (AFWA) modifications (LeGrand et al., 2019).

S1.3 Calculation of public health impacts

The relative risk of disease at a specific ambient $PM_{2.5}$ exposure was estimated through the Global Exposure Mortality Model (GEMM) (Burnett et al., 2018). The population attributable fraction (PAF) was estimated per grid cell as a function of population (P) and the relative risk (RR) of exposure following Equation 1. We used the GEMM for non–accidental mortality (non–communicable disease, NCD, plus lower respiratory infections, LRI), using parameters including the China cohort (Yin et al., 2017), with age–specific modifiers for adults over 25 years of age in 5–year intervals. The GEMM functions have mean, lower, and upper uncertainty intervals. The minimum-risk exposure for the GEMM functions is 2.4 µg m^{-3}.

$$PAF = P \times (RR_{EXP} - 1/RR_{EXP}) \tag{1}$$

For ambient ozone (O_3) exposure, the PAF was estimated as a function of the summary hazard ratio (HR) for chronic obstructive pulmonary disease (COPD) only and the change in annual average, daily maximum, 8–hour, O_3 concentrations (ADM8h) relative to the minimum–risk exposure (ΔX) as shown by Equation 2. The HR for COPD was 1.14 (95UI: 1.08–1.21) (Turner et al., 2016). The minimum-risk exposure followed the minimum percentiles of 26.7 ppb.

$$PAF = P \times \left(1 - e^{\Delta X \times ln(HR)/10}\right) \tag{2}$$

Premature mortality (MORT), years of life lost (YLL), and years lived with disability (YLD) per health outcome, age bracket, and grid cell were estimated as a function of the PAF and corresponding baseline mortality (I) following Equations 3, 4, and 5, respectively. Disability–adjusted life years (DALYs), i.e., the total loss of healthy life, were estimated as the total of YLL and YLD following Equation 6. Mean estimates were quantified in addition to upper and lower uncertainty intervals at the 95% confidence level. The rates of MORT, YLL, YLD, and DALYs were calculated per 100,000 population.

$$MORT = PAF \times I_{MORT} \tag{3}$$

$$YLL = PAF \times I_{YLL} \tag{4}$$

$$YLD = PAF \times I_{YLD} \tag{5}$$

$$DALYs = YLL + YLD \tag{6}$$

The United Nations adjusted population count dataset for 2015 at 0.25° × 0.25° resolution was obtained from the Gridded Population of the World, Version 4 (GPWv4) (Center for International Earth Science Information Network (CIESIN), 2016a). Population age composition for 2015 for adults 25 to 80 years in 5–year intervals, and 80 years plus, was taken from the Global Burden of Disease (GBD) Study 2017 (GBD 2017 Risk Factors Collaborators, 2018). Cause–specific (NCD, LRI, and COPD) baseline mortality and morbidity rates for 2015 for MORT, YLL, and YLD for each age bracket were also taken from the GBD Study 2017 (Institute for Health Metrics and Evaluation, 2019). Shapefiles were used to aggregate results at the country and state level (Hijmans et al., 2016).

S1.4 Measurements of particulate matter and ozone concentrations

To evaluate model-simulated monthly mean surface PM_{10} concentrations (Sects. 3.2.1 and 3.2.2), we used data from the Pollution Control Department (PCD) of the Thailand Government Ministry of Natural Resources and Environment (http://www.pcd.go.th/index.cfm). The PCD air quality database (available at: http://air4thai.pcd.go.th/webV2/history/) contains historical monthly mean PM_{10} concentrations measured at ground-based air quality monitoring stations located across Thailand (see Fig. S1a). To evaluate the GLOMAP model we used measurements from stations with data available between January 2003 and December 2015 (inclusive). To evaluate the WRF-Chem model we used measurements from stations with data available between January 2014 and December 2014 (inclusive).

To evaluate WRF-Chem-simulated surface ozone concentrations (Sect. 3.2.3), we used data from the Berkley Earth China Air Quality Data Set (available at: http://berkeleyearth.lbl.gov/manual/china_air_quality/) (Rohde and Muller, 2015). This dataset consists of hourly real-time ozone data recorded at surface air quality monitoring stations located in urban areas in China and surrounding countries (see Fig. S1b). The ozone data was downloaded by Rohde and Muller (2015) from https://aqicn.org/ between 5th April and 18th July 2014. Some quality control and validation checks were applied to the raw data prior to incorporation into the Berkley Earth China Air Quality Data Set (see further details in Rohde and Muller (2015)). We calculated daily mean values from the hourly data.

To evaluate WRF-Chem-simulated surface $PM_{2.5}$ concentrations (Sect. S2.2), we used a subset of measured annual mean $PM_{2.5}$ concentrations from the World Health Organization (WHO) Global Ambient Air Quality Database (WHO, 2018). The database consists of city-average annual mean $PM_{2.5}$ concentrations obtained from multiple ground station measurements across different years. To compare with the model concentrations, we selected measurement years to match or to be as close as possible to the simulation year of 2014. For some locations, $PM_{2.5}$ concentrations have been calculated by the WHO from the measured PM_{10} concentration using national conversion factors ($PM_{2.5}/PM_{10}$ ratio) either provided by the country or estimated as population-weighted averages of urban-specific conversion factors (estimated as the mean $PM_{2.5}/PM_{10}$ ratio of stations for the same year) for the country (WHO, 2016; 2018).

Prior to all model-measurement comparisons, simulated surface PM/ozone concentrations were linearly interpolated to the location (longitude and latitude) of the individual air quality monitoring stations; averaged over the corresponding time period (daily, monthly or annual); and simulated data corresponding to time periods of missing measurement data was removed.

S1.5 Global Subnational Infant Mortality Rates

We used the Global Subnational Infant Mortality Rates (IMR), Version 2, dataset from NASA Socioeconomic Data and Applications Center (SEDAC) (CIESIN, 2018a; Fig. S8), which is benchmarked to the year 2015. We selected the year 2015 (from two years available: 2000 and 2015) to be as close as possible to the WRF-Chem model simulation year (2014) and to be consistent with the 2015 population count dataset used to calculate public health impacts (Sect. S1.3). National median estimates of IMR show little change between 2014 and 2015 (ranging from a 1% change in Vietnam to an 8% change in China) (United Nations Inter-agency Group for Child Mortality Estimation, 2020).

The dataset includes IMR data for the lowest administrative units available for each country as of June 2017 (CIESIN, 2018b) at a spatial resolution of 30 arc-seconds (~1 km). The data were drawn from national offices, Demographic and Health Surveys (DHS), Multiple Indicator Cluster Surveys (MICS), and other sources from 2006 to 2014 (CIESIN, 2018b), with boundary inputs from the GPWv4 (CIESIN, 2016a; CIESIN, 2016b).

S2. Extended model evaluation

S2.1 Extended evaluation of GLOMAP fire-derived PM_{10}

Figure S2 summarises the agreement between the average seasonal cycles in GLOMAP-simulated and measured fire-derived PM_{10} concentrations at each of the 12 fire-influenced monitoring stations. The temporal correlation at each station is similar between the model simulations with fire (GFED: r=0.90-0.97; GFAS: r=0.80-0.93; FINN: r=0.80-0.99), but the observed magnitude and variability in monthly mean PM_{10} concentrations are captured best in the simulation with FINN emissions (GFED: normalised standard deviation (NSD)=0.25-0.37; GFAS: NSD=0.29-0.42; FINN: NSD=0.73-1.06).

S2.2 Evaluation of WRF-Chem $PM_{2.5}$

We evaluate annual mean $PM_{2.5}$ concentrations simulated by WRF-Chem because the estimated public health impacts of fire-derived PM (Sect. 3.4) are calculated using this quantity. Figure S5 compares annual mean surface $PM_{2.5}$ concentrations from the FINNx1.5 simulation against $PM_{2.5}$ measurements from the WHO Global Air Quality Database. The model captures the spatial distribution of measured annual mean $PM_{2.5}$ concentrations reasonably well across the region, with greatest concentrations in southern China and north-eastern India and comparatively lower concentrations over Mainland Southeast Asia (Fig. S5a). We find that the spatial agreement between the model and measurements (Fig 5b; r=0.47) is improved with 2014-only measurements (r=0.85) or only using direct measurements of $PM_{2.5}$, removing those converted from PM_{10} (r=0.86).

Simulated annual mean $PM_{2.5}$ concentrations are unbiased when compared against all the WHO measurements available within the model domain (Fig. S5b; NMBF=0.05). Table S1 summarises the agreement between model and measurements by country. The model captures the magnitude concentrations within a factor 1.5 in Vietnam, north-east India, southern China and Thailand. The model underestimates measured annual mean $PM_{2.5}$ concentrations in Myanmar by a factor 2 (NMBF=-1.01), likely due to a combination of underestimating anthropogenic and fire emissions, underestimating or missing outflow of PM from India, and mismatching measurement and simulation years. We also note that the WHO $PM_{2.5}$ concentrations reported for Myanmar are converted from PM_{10}, which can be associated with large uncertainties.

Supporting Tables

Country	No. of stations	Year(s) of measurements	Measured/ converted $PM_{2.5}$	Model (FINN) NMBF; r	Model (FINNx1.5) NMBF; r
South-eastern China	58	2014	Measured	+0.19; 0.86	+0.20; 0.86
North-eastern India	17	2012, 2014, 2015	Measured: 3 Converted: 14	+0.03; 0.26	+0.07; 0.28
Myanmar	16	2009, 2012, 2013, 2015	Converted	-1.23; 0.35	-1.01; 0.36
Thailand	22	2014	Converted	+0.09; 0.41	+0.16; 0.40
Vietnam	2	2016	Measured	+0.47; -	+0.50; -

Table S1. Summary of annual mean $PM_{2.5}$ measurements from the World Health Organization (WHO) Ambient Air Quality Database (WHO, 2018). The table shows the number of stations with available data, the year(s) the measurements were conducted and the number of reported $PM_{2.5}$ concentrations that were converted from PM_{10} measurements. The WRF-Chem normalised mean bias factor (NMBF; Yu et al., 2006) and Pearson's correlation coefficient (r) against observations are given for each country with available WHO measurements.

Country/ region	Reduction in $PM_{2.5}$ MORT	$PM_{2.5}$ MORT (yr^{-1})	$PM_{2.5}$ DALYs (yr^{-1})	Reduction in O_3 MORT	O_3 MORT (yr^{-1})
Cambodia	10%	1,100 (1,000-1,300)	44,500 (36,700-53,600)	15%	150 (130-160)
Laos	22%	1,200 (1,000-1,400)	47,600 (37,000-57,900)	17%	80 (70-90)
Myanmar	17%	8,000 (7,100-9,000)	293,800 (243,800-349,200)	21%	1,090 (960-1,210)
Thailand	12%	6,500 (6,000-7,000)	264,200 (221,300-311,100)	8%	620 (570-670)
Vietnam	3%	3,600 (3,300-4,100)	131,900 (108,800-159,100)	5%	410 (360-450)
Total Mainland SE Asia	9%	20,500 (18,400-22,700)	782,000 (647,700-931,000)	10%	2,350 (2,090-2,570)
SE China	3%	24,000 (23,400-24,800)	798,100 (703,500-906,800)	2%	2,170 (1,950-2,350)

Table S2. Averted public health effects due to changes in long-term exposure to ambient $PM_{2.5}$ and ozone (O_3) from eliminating fire emissions. Shown are the percentage reductions in annual disease burden, and the numbers of averted annual premature mortalities (MORT) and disability-adjusted life years (DALYs) per country for the lower fire emissions scenario (FINN). Values in parentheses represent the 95% uncertainty intervals (95UI). $PM_{2.5}$ mortality values are rounded to the nearest 100 and O_3 mortality values are rounded to the nearest 10. "SE China" is defined as south of 30°N and east of 98°W, and includes Hong Kong SAR, Macau SAR and Taiwan. "Mainland SE Asia" includes Cambodia, Laos, Myanmar, Thailand, and Vietnam.

Supporting Figures

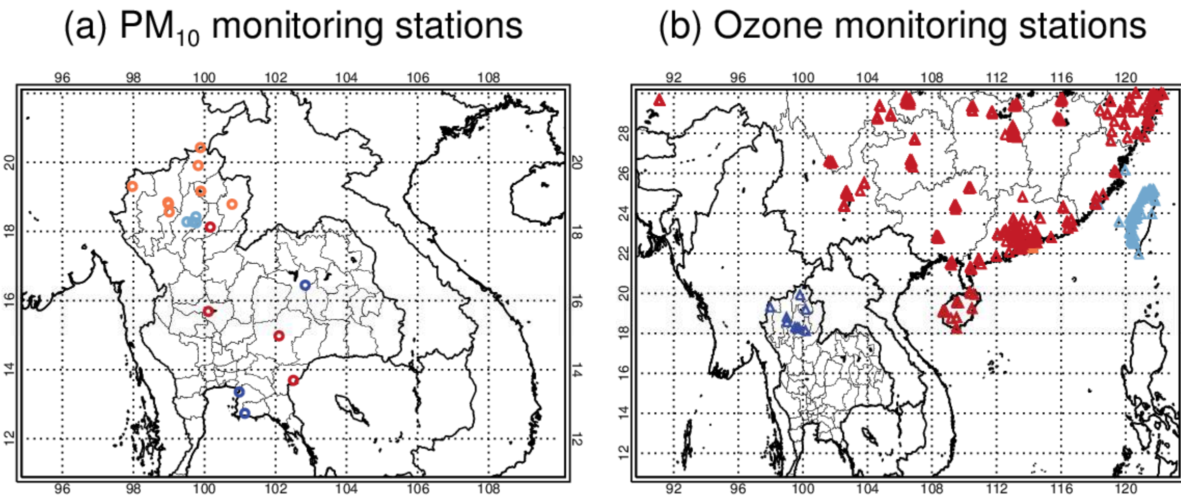

Figure S1. Locations of the air quality monitoring stations used to evaluate the models (Sects. 3.2 and 3.3). **(a)** Thailand PCD PM10 monitoring stations. Stations defined as influenced by fire emissions (where FINN fire-derived PM10 contribute ≥ 20% to the annual mean PM10) by both the GLOMAP and WRF-Chem models are coloured orange; Stations defined as fire-influenced by the WRF-Chem model only are coloured red; stations defined as fire-influenced by the GLOMAP model only are coloured light blue; the remaining stations are coloured dark blue. **(b)** Ozone monitoring stations from Rohde and Muller (2015) coloured by region: Thailand (dark blue); Mainland China (red); Hong Kong (orange); and Taiwan (light blue).

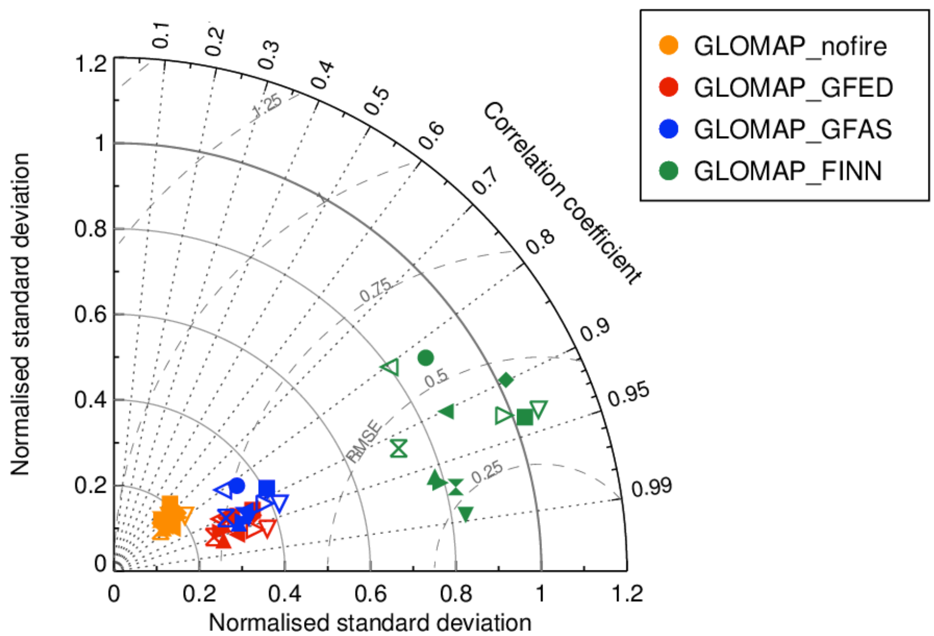

Figure S2. Taylor diagram comparing GLOMAP-simulated and measured multi-annual average seasonal cycles of fire-derived PM_{10} concentrations at 12 air quality monitoring stations in northern Thailand (Fig. S1). The measurements are represented by a point on the x-axis at unit distance from the y-axis. Results are shown for three model simulations: without fire emissions (GLOMAP_nofire); with GFED4 emissions (GLOMAP_GFED); with GFASv1.2 emissions (GLOMAP_GFAS); and with FINNv1.5 emissions (GLOMAP_FINN). The model standard deviation and centred root mean square error (RMSE) are normalised by dividing by the corresponding measured standard deviation. The normalised standard deviation and RMSE values are marked by the solid and dashed lines, respectively.

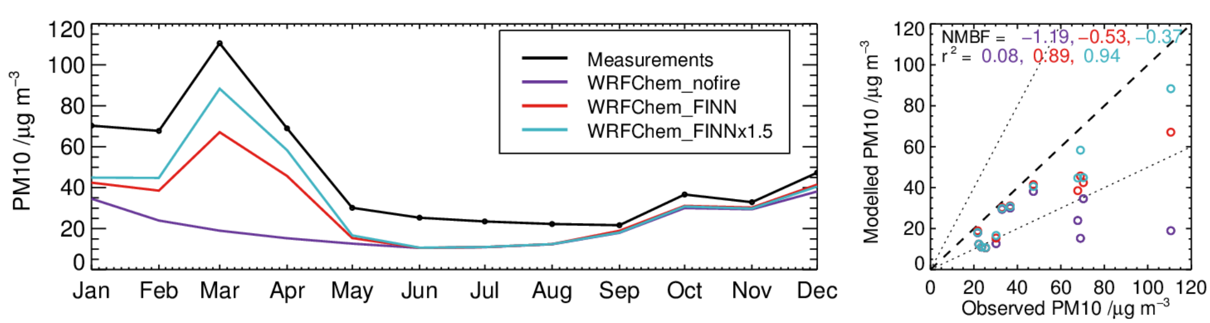

Figure S3. WRF-Chem-simulated and measured monthly mean *total* PM_{10} concentrations during 2014 averaged over 12 air quality monitoring stations in fire-influenced regions of Thailand (Fig. S1). Simulated concentrations are shown for the model without fire emissions (WRFChem_nofire), and for the model with FINN fire emissions (WRFChem_FINN) and with FINN emissions scaled upwards by a factor 1.5 (WRFChem_FINNx1.5).

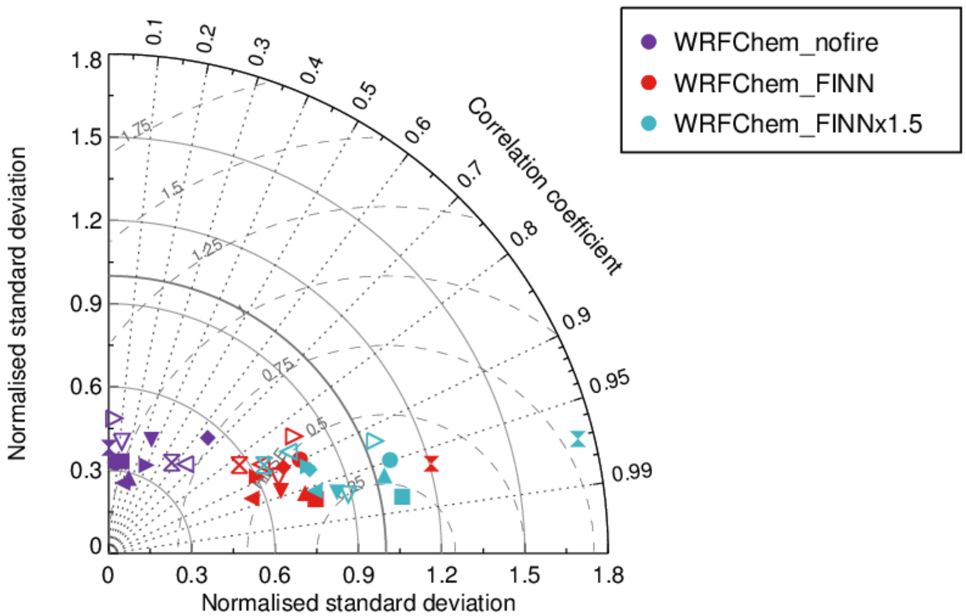

Figure S4. Taylor diagram comparing WRF-Chem-simulated and measured monthly mean fire-derived PM_{10} concentrations during 2014 at 12 air quality monitoring stations in fire-influenced regions of Thailand (Fig. S1). The measurements are represented by a point on the x-axis at unit distance from the y-axis. Results are shown for three model simulations: without fire emissions (WRFChem_nofire); with FINN fire emissions (WRFChem_FINN); and with FINN emissions scaled upwards by a factor 1.5 (WRFChem_FINNx1.5). The model standard deviation and centred root mean square error (RMSE) are normalised by dividing by the corresponding measured standard deviation. The normalised standard deviation and RMSE values are marked by the solid and dashed lines, respectively.

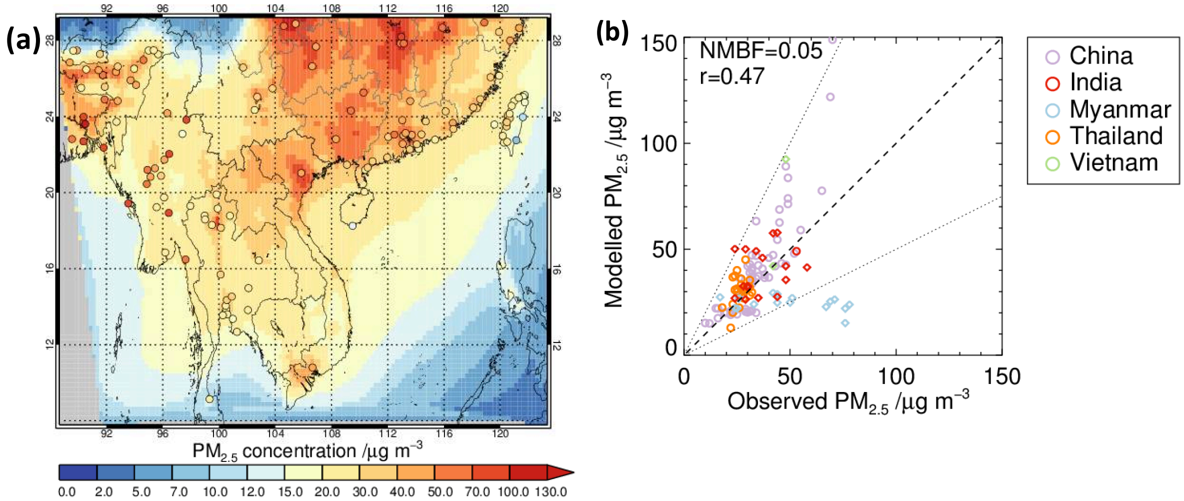

Figure S5. WRF-Chem-simulated and measured annual mean surface $PM_{2.5}$ concentrations across Southeast Asia. **(a)** Map of the simulated surface distribution of annual mean $PM_{2.5}$ for 2014 (underlying colours); overlying circles show measured annual mean $PM_{2.5}$ concentrations for available years (2009-2016). Regions in grey are outside the model domain. **(b)** Simulated versus measured annual mean $PM_{2.5}$ concentrations. Circles show measured annual mean $PM_{2.5}$ concentrations for the year 2014; diamonds show measured concentrations for years other than 2014. All simulated annual mean $PM_{2.5}$ concentrations are for the year 2014. The normalised mean bias factor (NMBF) and Pearson's correlation coefficient (r) between simulated and measured values are displayed in the top left corner.

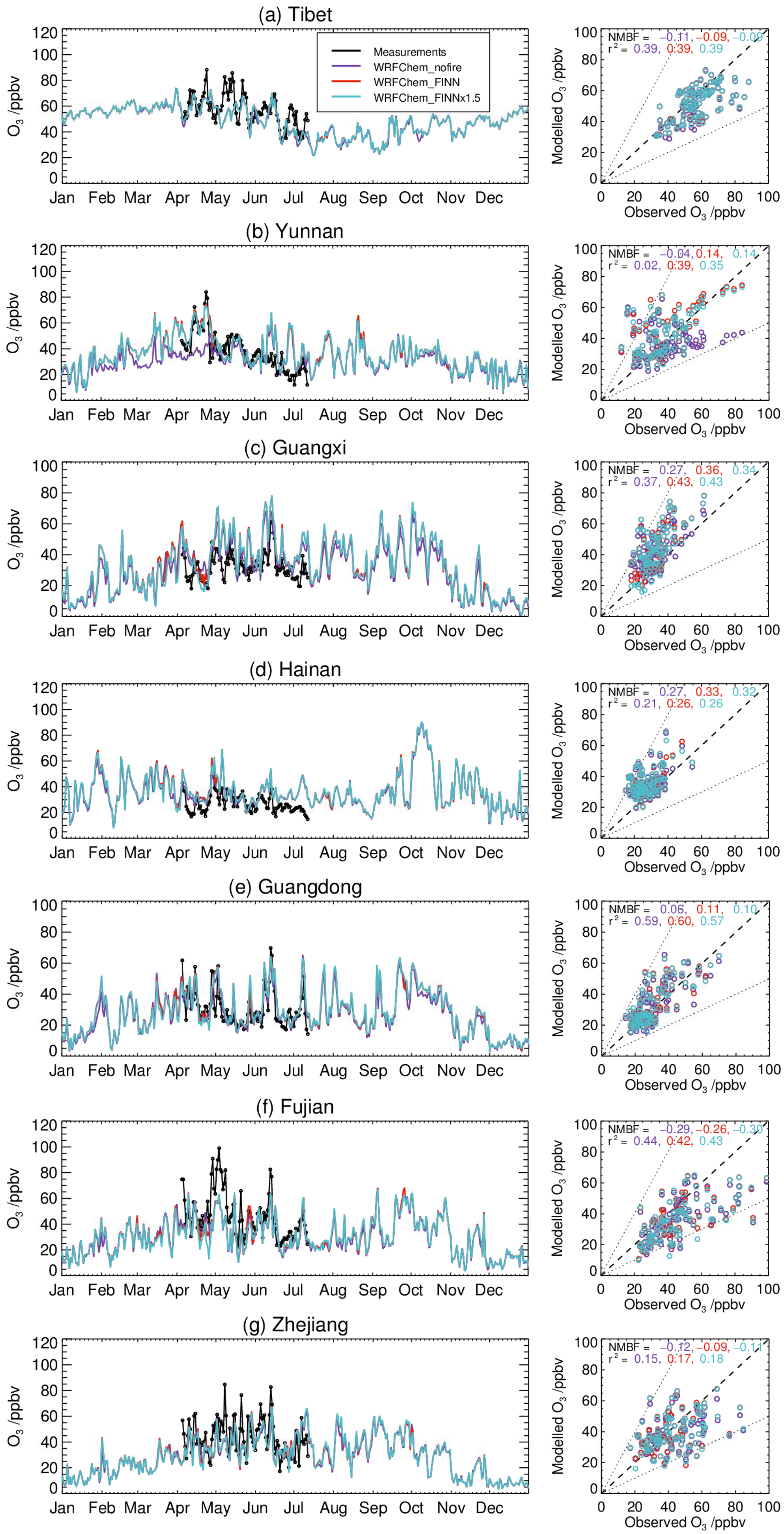

(a) Tibet
Measurements
WRFChem_nofire
WRFChem_FINN
WRFChem_FINNx1.5
NMBF = −0.11, −0.09,
r² = 0.39, 0.39, 0.39
(b) Yunnan
NMBF = −0.04, 0.14, 0.14
r² = 0.02, 0.39, 0.35
(c) Guangxi
NMBF = 0.27, 0.36, 0.34
r² = 0.37, 0.43, 0.43
(d) Hainan
NMBF = 0.27, 0.33, 0.32
r² = 0.21, 0.26, 0.26
(e) Guangdong
NMBF = 0.06, 0.11, 0.10
r² = 0.59, 0.60, 0.57
(f) Fujian
NMBF = −0.29, −0.26,
r² = 0.44, 0.42, 0.43
(g) Zhejiang
NMBF = −0.12, −0.09, −0.11
r² = 0.15, 0.17, 0.18
O3 /ppbv
Modelled O3 /ppbv
Observed O3 /ppbv
Jan Feb Mar Apr May Jun Jul Aug Sep Oct Nov Dec

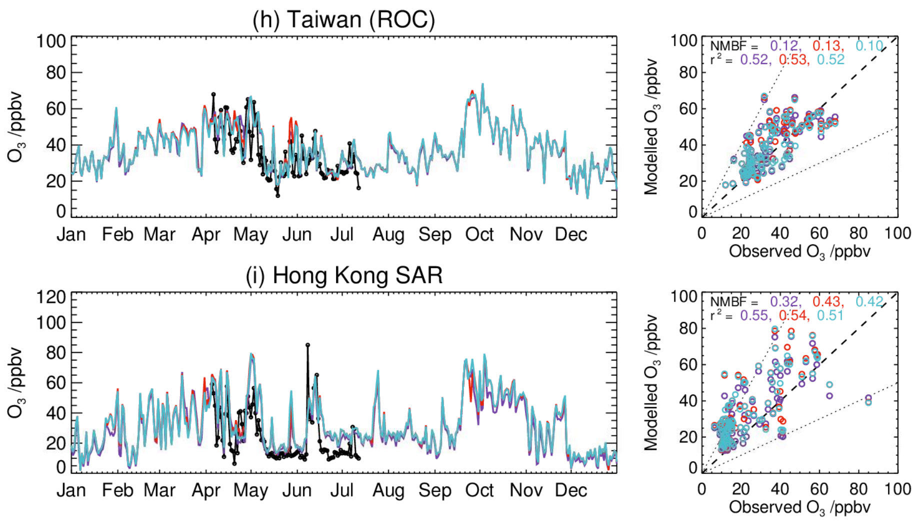

Figure S6. Evaluation of WRF-Chem-simulated ozone (O_3) over Thailand and South-eastern (SE) China. Left: Time-series of simulated and measured daily mean surface O_3 mixing ratios during 2014; Right: simulated versus measured daily mean O_3. Regional/province averages are shown for: **(a)** Tibet (7 air quality monitoring stations); **(b)** Yunnan (15 stations); **(c)** Guangxi (24 stations); **(d)** Hainan (20 stations); **(e)** Guangdong (113 stations); **(f)** Fujian (13 stations); **(g)** Zhejiang (60 stations); **(h)** Taiwan/Republic of China (ROC) (72 stations); and **(i)** Hong Kong Special Administrative Region (SAR) (12 stations). O_3 measurements are available from April to July 2014. The model bias (NMBF) and correlation (r^2) between modelled and measured values are given at the top of the righthand figures. Simulated values are shown for three model simulations: without fire emissions (WRFChem_nofire); with FINN fire emissions (WRFChem_FINN); and with FINN emissions scaled upwards by a factor 1.5 (WRFChem_FINNx1.5).

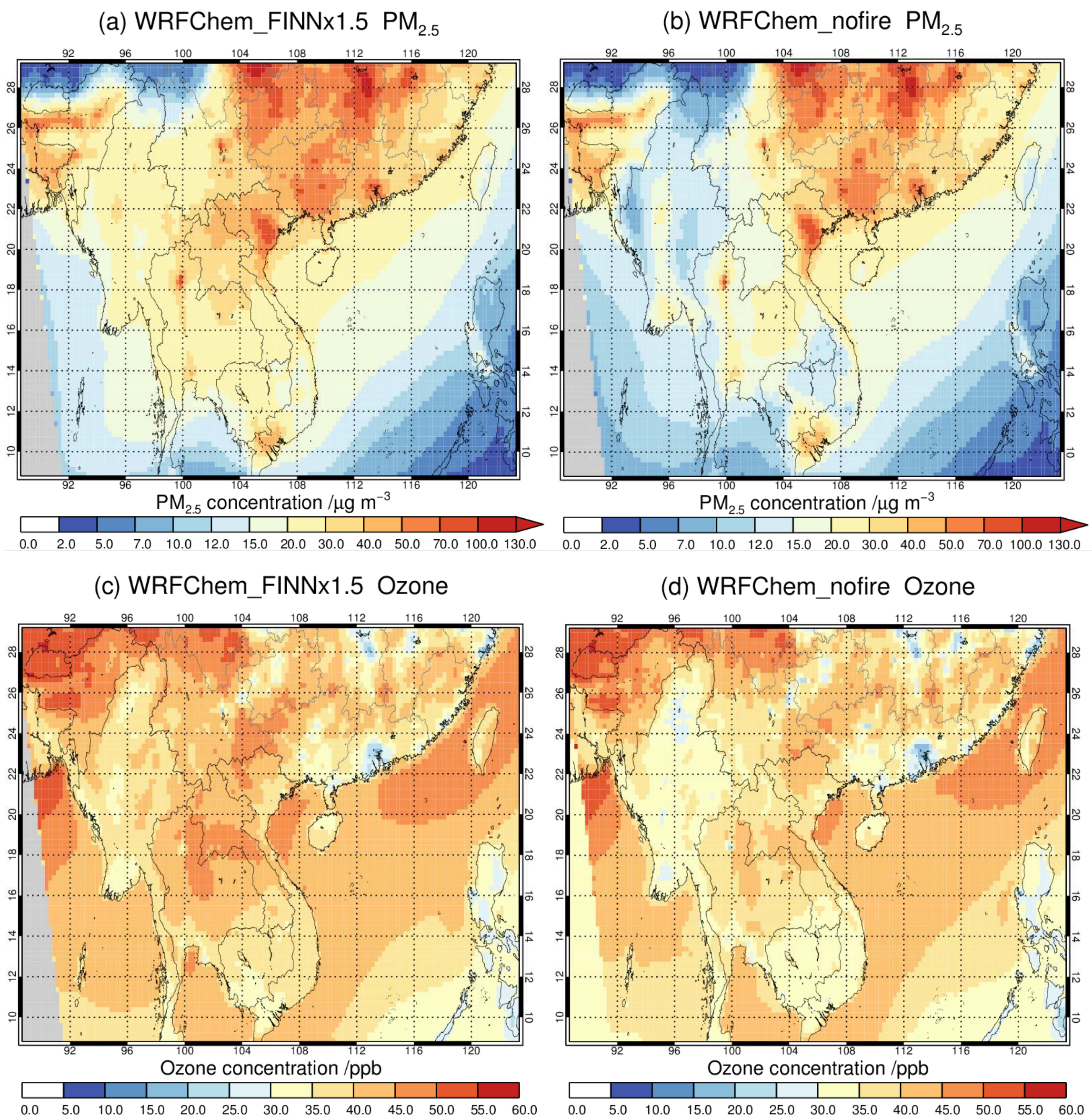

Figure S7. Spatial distribution of WRF-Chem-simulated annual mean surface **(a)** $PM_{2.5}$ and **(c)** ozone concentrations across Southeast Asia for 2014. Simulated concentrations are shown for the model simulation with FINN emissions scaled upwards by a factor 1.5 (WRFChem_FINNx1.5) in (a) and (c), and the model simulation without fire emissions (WRFChem_nofire) in **(b)** and **(d)**. Regions in grey are outside the model domain.

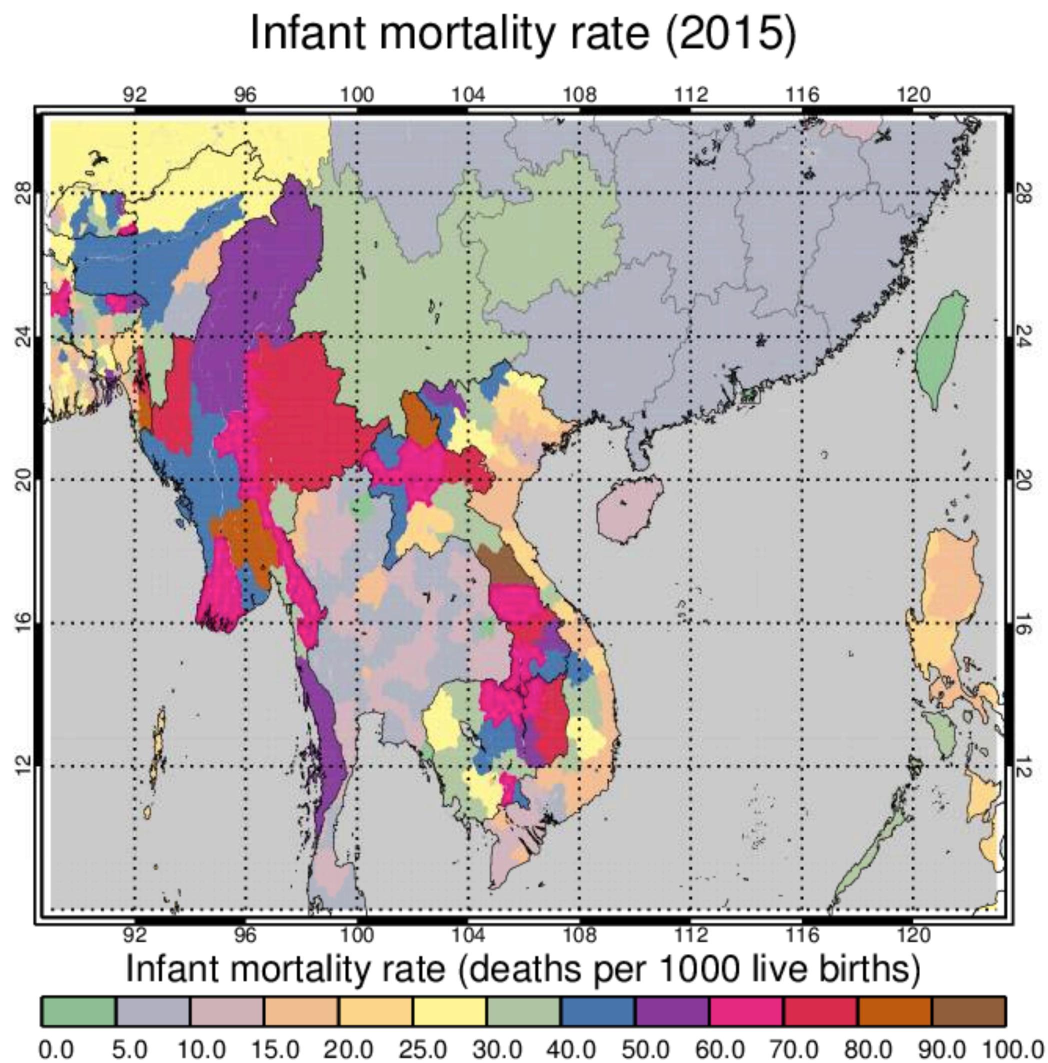

Figure S8. Spatial distribution of subnational infant mortality rate (IMR) estimates across Southeast Asia for the year of 2015 (CIESIN, 2018a). The gridded IMR estimates are at a spatial resolution of 30 arc-seconds (~1 km). The IMR for a region or country is defined as the number of children who die before their first birthday for every 1,000 live births.

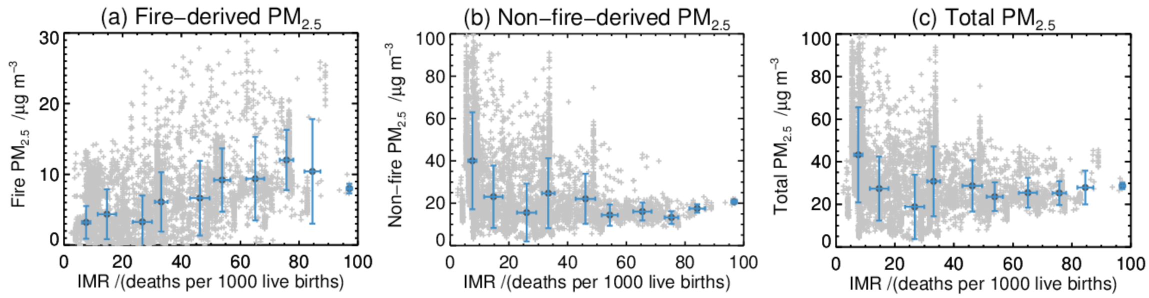

Figure S9. Gridded subnational Infant Mortality Rate (IMR; CIESIN, 2018a) values versus WRF-Chem simulated annual mean **(a)** fire-derived $PM_{2.5}$, **(b)** non-fire-derived $PM_{2.5,}$ and **(c)** total $PM_{2.5}$ concentrations across the Southeast Asian domain. The blue data points show mean values for binned IMR data (bin size = 10 deaths per 1,000 live births); error bars show the standard deviation. The grey data points show all 0.25°x0.25° grid cell values across the domain.

References

Arnold, S. R., Chipperfield, M. P., and Blitz, M. A.: A three dimensional model study of the effect of new temperature dependent quantum yields for acetone photolysis, J. Geophys. Res., 110, D22305, doi:10.1029/2005JD005998, 2005.

Balk, D., G. D. Deane, M. A. Levy, A. Storeygard, and S. Ahamed. 2006. The Biophysical Determinants of Global Poverty: Insights from an Analysis of Spatially Explicit Data. Paper presented at the 2006 Annual Meeting of the Population Association of America, Los Angeles, CA, 30 March-1 April 2006.

Burnett, R., Chen, H., Szyszkowicz, M., Fann, N., Hubbell, B., Pope Iii, C.A., Apte, J.S., Brauer, M., Cohen, A., Weichenthal, S., Coggins, J., Di, Q., Brunekreef, B., Frostad, J., Lim, S.S., Kan, H., Walker, K.D., Thurston, G.D., Hayes, R.B., Lim, C.C., Turner, M.C., Jerrett, M., Krewski, D., Gapstur, S.M., Diver, W.R., Ostro, B., Goldberg, D., Crouse, D.L., Martin, R.V., Peters, P., Pinault, L., Tjepkema, M., van Donkelaar, A., Villeneuve, P.J., Miller, A.B., Yin, P., Zhou, M., Wang, L., Janssen, N.A.H., Marra, M., Atkinson, R.W., Tsang, H., Quoc Thach, T., Cannon, J.B., Allen, R.T., Hart, J.E., Laden, F., Cesaroni, G., Forastiere, F., Weinmayr, G., Jaensch, A., Nagel, G., Concin, H., and Spadaro, JV.: Global estimates of mortality associated with longterm exposure to outdoor fine particulate matter, Proc. Natl. Acad. Sci. U.S.A., 115 (38), 9592-9597, doi: 10.1073/pnas.1803222115, http://www.pnas.org/content/pnas/115/38/9592.full.pdf, 2018.

Chipperfield, M. P.: New version of the TOMCAT/SLIMCAT offline chemical transport model: Intercomparison of stratospheric tracer experiments, Q. J. Roy. Meteor. Soc., 132, 1179–1203, 2006.

CIESIN (Center for International Earth Science Information Network), Columbia University. Gridded Population of the World, Version 4 (GPWv4): Population Count. Palisades, NY: NASA Socioeconomic Data and Applications Center (SEDAC). https://doi.org/10.7927/H4X63JVC, 2016a.

CIESIN (Center for International Earth Science Information Network), Columbia University. Gridded Population of the World, Version 4 (GPWv4): Land and Water Area. Palisades, NY: NASA Socioeconomic Data and Applications Center (SEDAC). https://doi.org/10.7927/H45M63M9, 2016b.

CIESIN (Center for International Earth Science Information Network), Columbia University. Global Subnational Infant Mortality Rates, Version 2. Palisades, NY: NASA Socioeconomic Data and Applications Center (SEDAC). https://doi.org/10.7927/H4PN93JJ, 2018a. Accessed: 2 November 2020.

CIESIN (Center for International Earth Science Information Network), Columbia University. Documentation for the Global Subnational Infant Mortality Rates, Version 2. Palisades, NY: NASA Socioeconomic Data and Applications Center (SEDAC). https://doi.org/10.7927/H44J0C25, 2018b.

Dee, D.P., Uppala, S.M., Simmons, A.J., Berrisford, P., Poli, P., Kobayashi, S., Andrae, U., Balmaseda, M.A., Balsamo, G., Bauer, P., Bechtold, P., Beljaars, A.C.M., van de

Berg, L., Bidlot, J., Bormann, N., Delsol, C., Dragani, R., Fuentes, M., Geer, A.J., Haimberger, L., Healy, S.B., Hersbach, H., Hólm, E.V., Isaksen, L., Kållberg, P., Köhler, M., Matricardi, M., McNally, A.P., Monge-Sanz, B.M., Morcrette, J.-J., Park, B.-K., Peubey, C., de Rosnay, P., Tavolato, C., Thépaut, J.-N. and Vitart, F. (2011), The ERA-Interim reanalysis: configuration and performance of the data assimilation system. Q.J.R. Meteorol. Soc., 137: 553-597. https://doi.org/10.1002/qj.828

Dentener, F., Kinne, S., Bond, T., Boucher, O., Cofala, J., Generoso,S., Ginoux, P., Gong, S., Hoelzemann, J. J., Ito, A., Marelli, L.,Penner, J. E., Putaud, J.-P., Textor, C., Schulz, M., van der Werf,G. R., and Wilson, J.: Emissions of primary aerosol and precur-sor gases in the years 2000 and 1750 prescribed data-sets for Ae-roCom, Atmos. Chem. Phys., 6, 4321–4344, doi:10.5194/acp-6-4321-2006, 2006.

Emmons, L. K., Walters, S., Hess, P. G., Lamarque, J.-F., Pfister, G. G., Fillmore, D., Granier, C., Guenther, A., Kinnison, D., Laepple, T., Orlando, J., Tie, X., Tyndall, G., Wiedinmyer, C., Baughcum, S. L., and Kloster, S.: Description and evaluation of the Model for Ozone and Related chemical Tracers, version 4 (MOZART-4), Geosci. Model Dev., 3, 43-67, https://doi.org/10.5194/gmd-3-43-2010, 2010.

GBD (Global Burden of Disease) 2015 Risk Factors Collaborators: Global, regional, and national comparative risk assessment of 79 behavioural, environmental and occupational, and metabolic risks or clusters of risks, 1990-2015: a systematic analysis for the Global Burden of Disease Study 2015, Lancet, 388, 1659–1724, https://doi.org/10.1016/S0140-6736(16)31679-8, 2016.

GBD (Global Burden of Disease) 2017 Risk Factors Collaborators: Global, regional, and national comparative risk assessment of 84 behavioural, environmental and occupational, and metabolic risks or clusters of risks for 195 countries and territories, 1990–2017: a systematic analysis for the Global Burden of Disease Study 2017, Lancet, 392, 1923–1994, DOI:https://doi.org/10.1016/S0140-6736(18)32225-6, 2018.

Granier, C., Bessagnet, B., Bond, T., D'Angiola, A., Denier van derGon, H., Frost, G. J., Heil, A., Kaiser, J. W., Kinne, S., Klimont,Z., Kloster, S., Lamarque, J.-F., Liousse, C., Masui, T., Meleux, F., Mieville, A., Ohara, T., Raut, J.-C., Riahi, K., Schultz, M.G., Smith, S. J., Thompson, A., Aardenne, J., van der Werf, G.R., and Vuuren, D. P.: Evolution of anthropogenic and biomass burning emissions of air pollutants at global and regional scales during the 1980–2010 period, Climatic Change, 109, 163–190, 2011.

Guenther, A., Hewitt, C. N., Erickson, D., Fall, R., Geron, C.,Graedel, T., Harley, P., Klinger, L., Lerdau, M., McKay, W. A.,Pierce, T., Scholes, B., Steinbrecher, R., Tallamraju, R., Taylor, J., and Zimmerman, P.: A global model of natural volatile organic compound emissions, J. Geophys. Res., 100, 8873–8892, 1995.

Guenther, A., Karl, T., Harley, P., Wiedinmyer, C., Palmer, P. I., and Geron, C.: Estimates of global terrestrial isoprene emissions using MEGAN (Model of Emissions of Gases and Aerosols from Nature), Atmos. Chem. Phys., 6, 3181-3210, https://doi.org/10.5194/acp-6-3181-2006, 2006.

Hijmans, R., University of California, Berkeley Museum of Vertebrate Zoology, Kapoor, J., Wieczorek, J., International Rice Research Institute, et al.: Global Administrative Areas (GADM): Boundaries without limits. Version 2.8, 2016.

Hodzic, A. and Jimenez, J. L.: Modeling anthropogenically controlled secondary organic aerosols in a megacity: a simplified framework for global and climate models. Geosci. Model Dev., 4, 901-917, 2011.

Hodzic, A. and Knote, C.: WRF-Chem 3.6.1: MOZART gas-phase chemistry with MOSAIC aerosols, Atmospheric Chemistry Division (ACD), National Center for Atmospheric Research (NCAR), 2014.

Institute for Health Metrics and Evaluation: Global Burden of Disease (GBD) Compare Data Visualization. Retrieved February 13, 2019, from https://vizhub.healthdata.org/gbd-compare/, 2019.

Janssens-Maenhout, G., Crippa, M., Guizzardi, D., Dentener, F., Muntean, M., Pouliot, G., Keating, T., Zhang, Q., Kurokawa, J., Wankmüller, R., Denier van der Gon, H., Kuenen, J. J. P., Klimont, Z., Frost, G., Darras, S., Koffi, B., and Li, M.: HTAP_v2.2: a mosaic of regional and global emission grid maps for 2008 and 2010 to study hemispheric transport of air pollution, Atmos. Chem. Phys., 15, 11411-11432, https://doi.org/10.5194/acp-15-11411-2015, 2015.

Knote, C., Hodzic, A., Jimenez, J. L., Volkamer, R., Orlando, J. J., Baidar, S., Brioude, J., Fast, J., Gentner, D. R., Goldstein, A. H., Hayes, P. L., Knighton, W. B., Oetjen, H., Setyan, A., Stark, H., Thalman, R., Tyndall, G., Washenfelder, R., Waxman, E., and Zhang, Q.: Simulation of semi-explicit mechanisms of SOA formation from glyoxal in aerosol in a 3-D model, Atmos. Chem. Phys., 14, 6213-6239, https://doi.org/10.5194/acp-14-6213-2014, 2014.

LeGrand, S. L., Polashenski, C., Letcher, T. W., Creighton, G. A., Peckham, S. E., and Cetola, J. D.: The AFWA dust emission scheme for the GOCART aerosol model in WRF-Chem v3.8.1, Geosci. Model Dev., 12, 131-166, https://doi.org/10.5194/gmd-12-131-2019, 2019.

Mann, G. W., Carslaw, K. S., Spracklen, D. V., Ridley, D. A., Manktelow, P. T., Chipperfield, M. P., Pickering, S. J., and Johnson, C. E.: Description and evaluation of GLOMAP-mode: a modal global aerosol microphysics model for the UKCA composition-climate model, Geosci. Model Dev., 3, 519-551, doi:10.5194/gmd-3-519-2010, 2010.

NCAR (National Center for Atmospheric Research): ACOM MOZART-4/GEOS-5 global model output. Available at: http://www.acom.ucar.edu/wrf-chem/mozart.shtml UCAR, 2016.

NCEP: National Weather Service, NOAA & U.S. Department of Commerce. NCEP Final (FNL) Operational Model Global Tropospheric Analyses, continuing from July 1999. Research Data Archive at the National Center for Atmospheric Research, Computational and Information Systems Laboratory, https://doi.org/10.5065/D6M043C6, 2000.

NCEP: National Weather Service, NOAA & U.S. Department of Commerce. NCEP Global Forecast System (GFS) Analyses and Forecasts. Research Data Archive at the National Center for Atmospheric Research, Computational and Information Systems Laboratory, http://rda.ucar.edu/datasets/ds084.6/, 2007.

Rohde, R. A. and Muller, R. A.: Air pollution in China: mapping of concentrations and sources, PLoS ONE, 10, 1-14, doi:10.1371/journal.pone.0135749, 2015.

Scott, C. E., Rap, A., Spracklen, D. V., Forster, P. M., Carslaw, K. S., Mann, G. W., Pringle, K. J., Kivekäs, N., Kulmala, M., Lihavainen, H., and Tunved, P.: The direct and indirect radiative effects of biogenic secondary organic aerosol, Atmos. Chem. Phys., 14, 447-470, https://doi.org/10.5194/acp-14-447-2014, 2014.

Spracklen, D. V., Pringle, K. J., Carslaw, K. S., Chipperfield, M. P., and Mann, G. W.: A global off-line model of size-resolved aerosol microphysics: I. Model development and prediction of aerosol properties, Atmos. Chem. Phys., 5, 2227-2252, doi:10.5194/acp-5-2227-2005, 2005.

Turner, M. C., Jerrett, M., Pope III, C. A., Krewski, D., Gapstur, S. M., Diver, R. W., et al.: Long-Term Ozone Exposure and Mortality in a Large Prospective Study. American Journal of Respiratory and Critical Care Medicine, 193(10), 1134–1142. https://doi.org/10.1164/rccm.201508-1633OC, 2016.

United Nations Inter-agency Group for Child Mortality Estimation: Infant mortality rate estimates developed by the United Nations Inter-agency Group for Child Mortality Estimation (UNIGME), 2020. Available at www.childmortality.org. Accessed: 5 May 2021.

World Health Organization (WHO): Ambient Air Pollution: A Global Assessment Of Exposure And Burden Of Disease, Vol. 121, World Health Organization, Geneva, 1–131, 2016.

World Health Organization (WHO): WHO Global Ambient Air Quality Database (update 2018) edition, Version 1.0, Geneva, World Health Organization, 2018. Available at: https://www.who.int/airpollution/data/cities/en/, last access: 1 August 2019.

Yin, P., Brauer, M., Cohen, A., Burnett, R. T., Liu, J., Liu, Y., et al.: Long-term fine particulate matter exposure and nonaccidental and cause-specific mortality in a large national cohort of Chinese men. Environmental Health Perspectives, *125*(11), 117002-1-117002–117011. https://doi.org/10.1289/EHP1673, 2017.

Zaveri, R. A., Easter, R. C., Fast, J. D. and Peters, L. K.: Model for Simulating Aerosol Interactions and Chemistry (MOSAIC), J. Geophys. Res. Atmos., 113, D13204, doi:10.1029/2007JD008782, https://doi.org/10.1029/2007JD008782, 2008.